

AUTHOR QUERY FORM

 ELSEVIER	Journal: VOLGEO Article Number: 4656	Please e-mail or fax your responses and any corrections to: E-mail: corrections.esnl@elsevier.spitech.com Fax: +1 619 699 6721
--	---	--

Dear Author,

Any queries or remarks that have arisen during the processing of your manuscript are listed below and highlighted by flags in the proof. Please check your proof carefully and mark all corrections at the appropriate place in the proof (e.g., by using on-screen annotation in the PDF file) or compile them in a separate list.

For correction or revision of any artwork, please consult <http://www.elsevier.com/artworkinstructions>.

Any queries or remarks that have arisen during the processing of your manuscript are listed below and highlighted by flags in the proof. Click on the 'Q' link to go to the location in the proof.

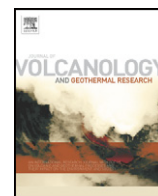
Location in article	Query / Remark: click on the Q link to go Please insert your reply or correction at the corresponding line in the proof
Q1	Country name for affiliation a is missing. Costa Rica is provided; please check if appropriate, and correct if necessary.
Q2	Please provide 3–5 Research Highlights (with a maximum 85 characters per bullet point, including spaces). For more information, see the Guide for Authors .
Q3	Citation “Macdonald (1973)” has not been found in the reference list. Please supply full details for this reference.
Q4	Citation “Bednardz and Schmincke, 1990” has not been found in the reference list. Please supply full details for this reference.
Q5	Citation “Bernarz and Schmincke, 1990” has not been found in the reference list. Please supply full details for this reference.
Q6	Citation “Guibaud et al., 2009” has not been found in the reference list. Please supply full details for this reference.
Q7	Fig. 14 was cited but only 12 figures were provided. Please check and correct if necessary.
Q8	Uncited reference: This section comprises references that occur in the reference list but not in the body of the text. Please position each reference in the text or, alternatively, delete it. Any reference not dealt with will be retained in this section. Thank you.

Thank you for your assistance.



Contents lists available at ScienceDirect

Journal of Volcanology and Geothermal Research

journal homepage: www.elsevier.com/locate/jvolgeores

The Cerro Chopo basaltic cone (Costa Rica): An unusual completely reversed graded pyroclastic cone with abundant low vesiculated cannonball juvenile fragments

Guillermo E. Alvarado^{a,b,*}, Wendy Pérez^{b,c}, Thomas A. Vogel^d, Heike Grüger^e, Lina Patiño^d

^a Área de Amenazas y Auscultación Sismovolcánica, Instituto Costarricense de Electricidad, Costa Rica

^b Escuela Centroamericana de Geología, Universidad de Costa Rica, Apdo. 35, San José, Costa Rica

^c RD 4 - Dynamics of the Ocean Floor, IFM-GEOMAR, Wischhofstr., 1-3, 24148 Kiel, Germany

^d Department of Geological Sciences, Michigan State University, East Lansing, MI 48824-1115, USA

^e Geological and Paleontological Institute, University of Basel, Bernoullistr. 32, 4056 Basel, Switzerland

ARTICLE INFO

Article history:

Received 24 March 2010

Accepted 3 November 2010

Available online xxx

Keywords:

pyroclastic cone

reverse grading

cannonball bombs

Cerro Chopo

Costa Rica

ABSTRACT

Cerro Chopo is a partially dissected, asymmetric, isolated Pleistocene pyroclastic cone, located in front of the Cordillera de Guanacaste, in northern Costa Rica. The cone consists of ~0.09 km³ of basaltic tephra, as well as ~0.14 km³ of lateral lava flows. Tephra are tholeiitic, high-alumina, olivine basalts, and represent minor degrees (≤5%) of crystal fractionation. Major and trace element compositions are consistent with minor fractionation from a mixture of E-MORB and OIB magmas. The cone walls consist of alternating coarser- and finer grained well-sorted beds, containing continuous spectra from breadcrust to smooth surface cannonball bombs, but also less frequent cylindrical fragments and broken clasts. Cerro Chopo is unique compared to other typical scoria cones because it contains ubiquitous reversely-graded layers, scarcity of scorias, and instead a wide range of dense (1.54–2.49 g/cm³) poorly vesicular (5–40 vol.%) juvenile **clast** morphologies, including abundant cannonball juvenile bombs and lapilli. These are bombs with concentric layers surrounding vesiculated, dense and lapillistone cores and are interpreted to have repeatedly recycled through the vent. The **cannonball** bombs and lapilli have been described in a few scoria cones but are much less abundant than in Chopo. The reverse graded sequences are interpreted to have resulted from decreasing explosivity at the vent, in addition to local failure of tephra on slopes as the consequence of grain flows. Elsewhere on the Earth, most of the poorly-vesiculated spherical bombs, particularly cannonball, accretionary, composite, and core bombs, and its equivalent lapilli size (pelletal, spinning droplets and ellipsoidal lapilli), are all related to mafic to ultramafic, low-viscosity magmas.

© 2010 Published by Elsevier B.V.

1. Introduction

Scoria, cinder, tephra or pyroclastic cones are one of the most common expressions of subaerial volcanism. They are relatively small in size (5–1000 m high; ratio high/wide: 1.1–1.9; usually 1.5–1.6), **slope** angles range between 25° and 35°, and are mostly related to Hawaiian and Strombolian eruptions of mafic to intermediate magmas (Breed, 1964; Wood, 1980; Fisher and Schmincke, 1984). They commonly form volcanic fields comprising hundreds of such cones, and form by near-surface expansion and explosive disruption of gas bubbles in magmas with relatively low viscosity. The physical evolution of these volcanic features has been documented by observation of historical eruptions, including the famous and well-recorded growth of Parícutín volcano (México) in 1943, and the historically most active cinder cone, Cerro Negro volcano in Nicaragua (e.g. Williams and McBirney, 1979;

McKnight and Williams, 1997). Growth models have been established from direct observations, laboratory experiments and theoretical studies (Blackburn et al., 1976; Vergnolle and Brandeis, 1996; Vergnolle et al., 1996 and references therein). Scoria cones are often monogenetic, being only active for less than a year, indicating a lack of large-scale magma bodies residing at some depth beneath the cone, and therefore their composition can be used to infer the nature of the mantle source (Wood, 1980).

The Cerro Chopo cone, located in northern Costa Rica (Fig. 1), has gone through extensive quarrying (Figs. 2 and 3) that exposed the internal structure of the cone. This deposit has two characteristics that make Chopo different from the majority of monogenetic cones elsewhere: 1) the rhythmic reverse grading of the layers present through the whole stratigraphic sequence from bottom to top, and 2) the abundance of poorly-vesicular cannonball juvenile fragments, ranging in size from coarse ash to bomb, containing different internal and rind structures which occur throughout the whole sequence. The predominance of high density, poorly vesicular juvenile fragments leads us to define Cerro Chopo as a pyroclastic cone and not as a cinder or scoria cone.

* Corresponding author. Área de Amenazas y Auscultación Sismológica y Volcánica, PySA, Instituto Costarricense de Electricidad (ICE) Apdo. 10032-1000, San José, Costa Rica. Tel.: +506 2220 8217.

E-mail address: galvarado@ice.go.cr (G.E. Alvarado).

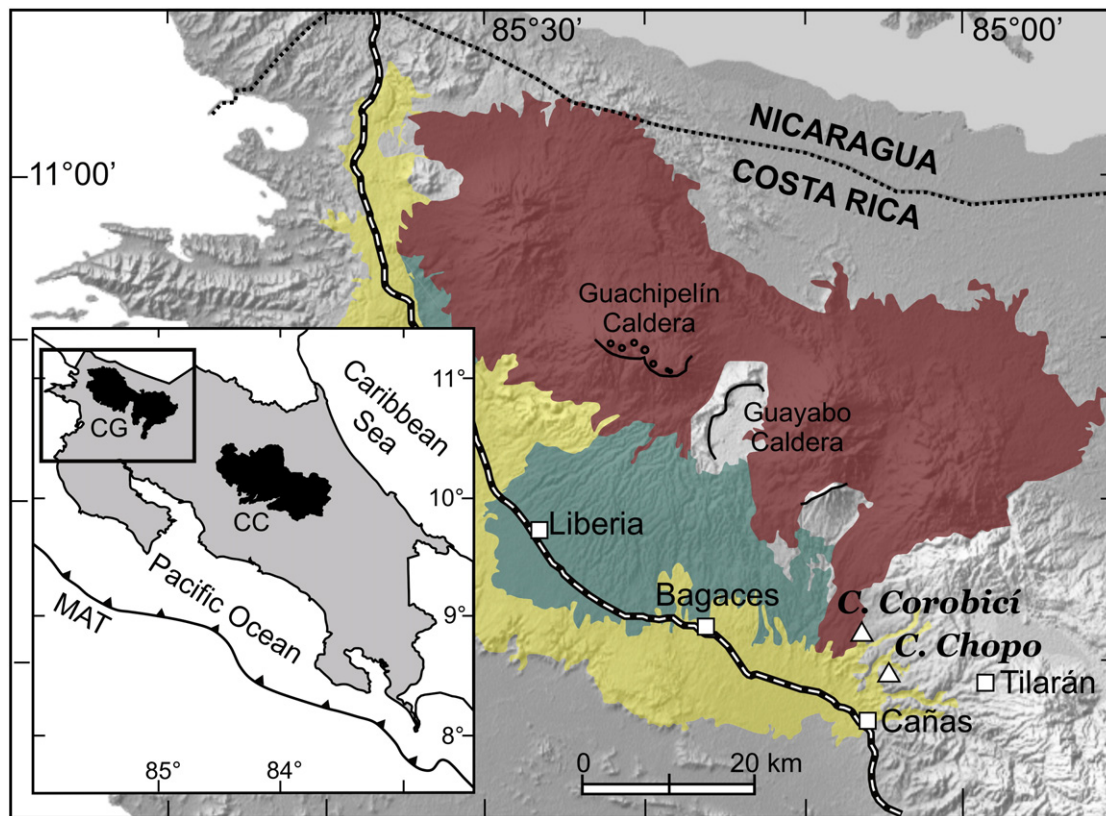


Fig. 1. Location and geological setting of the Cerro Chopo scoria cone (simplified after Denyer and Alvarado, 2007). The inset shows Costa Rica and its two volcanic ranges the Cordillera Central (CC) and the Cordillera de Guanacaste (CG). The last one is also shown in the shaded relief as the darker region. The middle gray area corresponds to the ignimbritic fan deposits (1.6–0.6 Ma) from two recent calderas, and the brightest gray is the Bagaces ignimbritic plateau (2–4 Ma). Cerro Corobicí scoria cone is also shown to the northwest of Cerro Chopo.

This paper describes the reverse grading and dense juvenile fragments, propose a mode of formation for their abundance. This is a key to understand this particular eruptive style that differs from typical Strombolian and Hawaiian deposits. Although massive, normal and reverse grading is a frequent feature in basaltic eruption styles (Valentine and Gregg, 2008), at Chopo this is pervasive all around the cone and from the base to top. We also make a brief compilation of the reported cases of spherical bombs (including the cannonball juvenile clasts and cored bombs, which is a type of pyroclastic fragments only reported in a few places in the world, their different geological contexts and interpretations).

2. Background

2.1. Grain size and grading

Grading in pyroclastic fall deposits, inverse or reverse in particular, can be attributed to variety of causes:

- (1) A decrease in gas content of the magma and therefore explosiveness (Macdonald, 1972).
- (2) A progressive increase in initial gas velocity or the density of the eruption column, or inclination of the eruption column during the eruption. Increasing gas velocity would eject larger fragments to greater heights in the later phases and promote a wider dispersal by the wind (Booth, 1973; Lirer et al., 1973). On the other hand, changes in eruption column density can increase the release height of individual large clasts from the column and, therefore, the range of dispersal of large clasts (Wilson, 1976). According to Houghton et al. (2000) changes in

the inclination of the eruption column or jet can also affect the gradation.

- (3) Change in the morphology of the eruptive conduit or vent as the eruption proceeds, for example from a cylindrical to a conical vent enables particles to be ejected at lower angles and therefore to travel farther in the near vent facies (Murata et al., 1966); or a widening of the conduit radius may reduce the frictional drag on the erupting gas and particles, thereby giving an increased exit velocity if the same mean gas velocity is maintained (Fisher and Schmincke, 1984).
- (4) External factors like changes in wind velocity and direction during eruption (Houghton et al., 2000), deposition in water (Bateman, 1953) or by frost heaving in cold climates (Fisher and Schmincke, 1984).
- (5) Slope instability at the time of deposition generating rolling of large clasts over smaller clasts on the surface of a steep slope, or down slope flow of a blanket of accumulating fragments on slopes at or near the angle of repose (Duffield et al., 1979).

2.2. Spherical-cannonball-cored bombs

Perhaps the first mention of a spherical bomb was made by Darwin (1845) when he visited in 1836 the volcanic island of Reunion in the central Atlantic on his way to the Galápagos Islands: "In several places I noticed volcanic bombs, that is, masses of lava which have been shot through the air whilst fluid, and have consequently assumed a spherical or pear-shape". Spherical bombs are relatively rare in monogenetic cones in comparison with the typical types of bombs like breadcrusted, cow-dung, cauliflower, ribbon, cylindrical fusiform and spindle or rugged bombs. However, the bombs described and drawn by Darwin were highly vesicular in contrast with those bombs

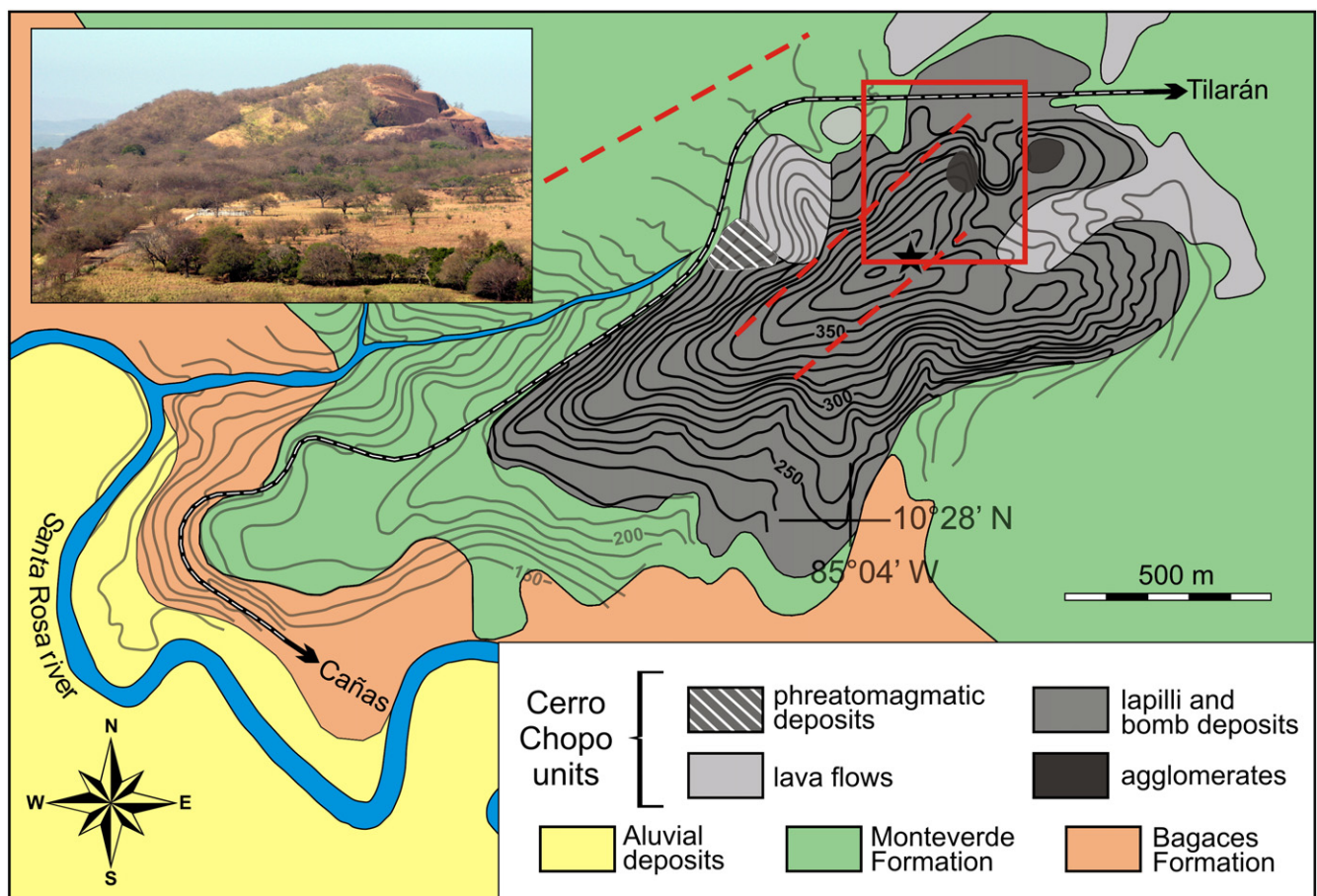


Fig. 2. Geological map of the Cerro Chopo cone modified after Mora (1977) and Ramírez and Umaña (1977). The lava flows are distributed to the northeast. The red quadrangle represents the area studied in detail and shown in Fig. 3, where the quarries are located. The star shows the position of the vent suggested by Mora (1977) and the red dashed lines are major faults. (For interpretation of the references to color in this figure legend, the reader is referred to the web version of this article.)

135 described in Cinder Cone (Lassen Volcanic National Park, California,
136 USA). These were called “spherical” by Macdonald (1972), who
137 proposed they were ejected as separated blebs tending to be pulled
138 into spheres, and “accretionary bombs” by Heiken (1978).

139 At Pacaya volcano (Guatemala) bombs were observed bouncing
140 down the slopes during the 1970 eruption. The bombs had a smoothly
141 rounded surface with a subspherical to prolate ellipsoid shape. Francis
142 (1973) called them “cannonball” and explained their shape as
143 originated as fragments of hot pasty lava rounded by mechanical
144 processes while traveling at high speed down the slopes. There was no
145 evidence of internal structures such as layering or cores of other rocks
146 (Francis, 1973). Rosseel et al. (2006) also used the term cannonball
147 bombs for subspherical (elliptical, asymmetrically flattened to oblate
148 disk shapes), some of them with breadcrusted or even rugged
149 cauliflower texture. Thus, there is a transition or major shape
150 tendencies from the spherical one (cannonball) to the rugged one
151 (see Rosseel et al., 2006). Other examples of spherical bombs have
152 been mentioned at the Calatrava field –called spheroidal bombs–
153 (Spain; Araña and López, 1974; Carracedo Sánchez et al., 2009), at the
154 Marteles maar (Gran Canaria; Schmincke, 1977; Schmincke and
155 Sumita, 2010) and 1949 Hoyo Negro scoria cone (La Palma, Canary
156 Islands; Schmincke and Sumita, 2010), at Pelagatos scoria cone in
157 México (Guilbaud et al., 2009), in Rothenberg scoria cone in the East
158 Eifel, Germany (Houghton and Schmincke, 1989), Montaña Rajada
159 cone (Timanfaya volcanic field, Lanzarote, Spain), and the present
160 case at Cerro Chopo. Because all of these clast types are petrographically
161 similar, they are interpreted to be comagmatic. The internal
162 structure shows that, in most cases, there is more than one coating

163 layer of juvenile basaltic lava, which can be interpreted as indicating
164 multiple cycles of ejection, recapture in the melt and re-eruption.

165 Another variety of spherical bomb consists of accidental rock
166 fragments or crystals (core) surrounded by a chilled shell or carapace
167 of quenched juvenile material. These are called “cored bombs” or
168 “cored juvenile clasts” and have been reported in Orlot, Gerona
169 (Spain; Araña and López, 1974), at the phreatomagmatic eruptions of
170 the 1886 Rotomahana eruption (Tarawera, New Zealand; Rosseel
171 et al., 2006) and in the Colli Albani Volcanic District (Italy; Sottili et al.,
172 2009, 2010). They record the thermal interaction of magma with wall
173 rocks.

174 Spherical clasts in the lapilli fraction size are described in the
175 literature as composite lapilli or ellipsoidal lapilli (Bednarz, 1982;
176 Fisher and Schmincke, 1984; Bednarz and Schmincke, 1990), pelletal
177 lapilli and spinning droplet (Lloyd and Stoppa, 2003), which could
178 have a certain structural and genetic analogy with those bombs
179 described before but are out of the scope of this study (for details see
180 Carracedo Sánchez et al., 2009).

181 There is a general agreement that spherical juvenile clasts are
182 associated with a mafic to ultramafic, low-viscosity magma with a
183 limited amount of water in an open system (Schmincke, 1977;
184 Heiken, 1978; Bednarz and Schmincke, 1990; Rosseel et al., 2006;
185 Carracedo Sánchez et al., 2009; Sottili et al., 2009, 2010), but the
186 model is still under discussion. Also, this type of spherical juvenile
187 products occurs in a few historical cases including an observed one (at
188 Pacaya volcano observed by Francis, 1973).

189 It is usually assumed that spheroidal bombs and lapilli are formed
190 through cooling of molten clots pulled up into spheres by the surface

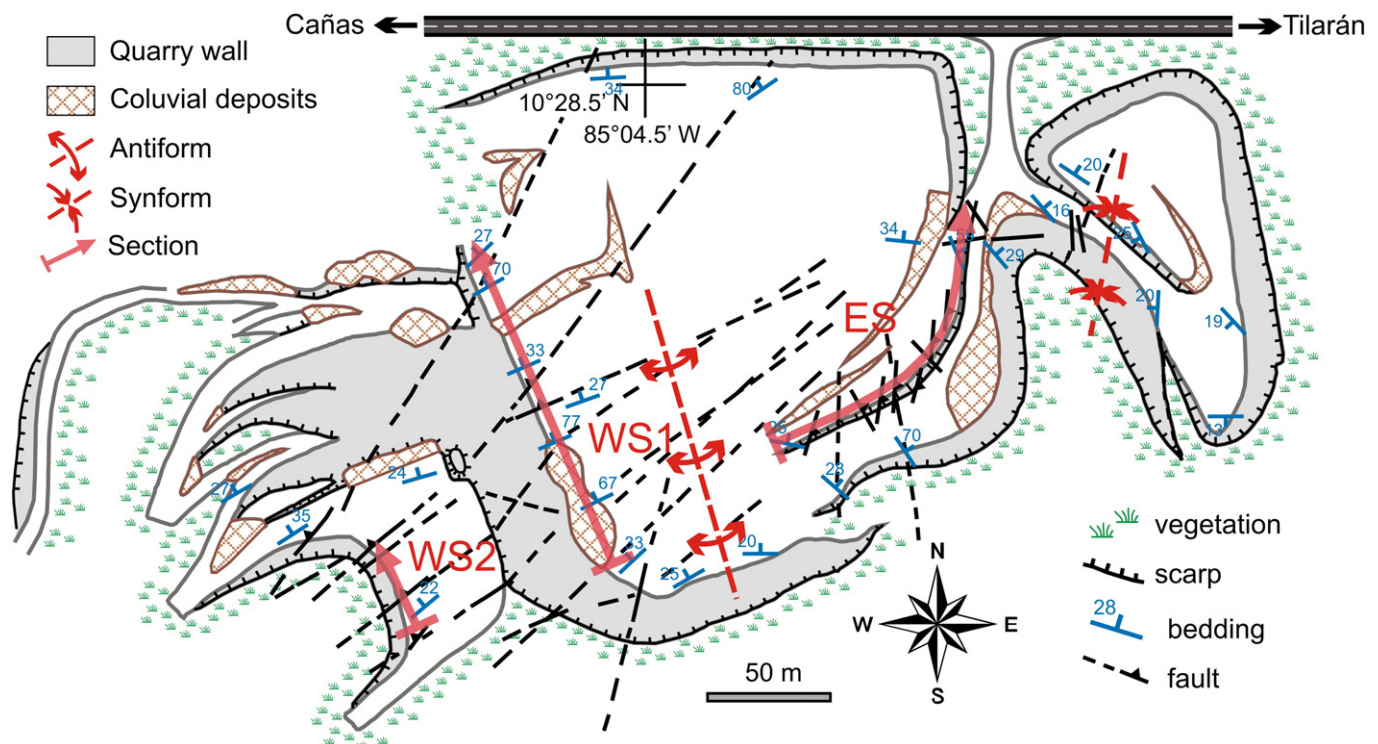


Fig. 3. Sketch of the quarry at Cerro Chopo showing by arrows the stratigraphical profiles used for correlation (and shown in Fig. 10), as well as the structural elements like bedding and faults. The red discontinuous lines point to the axis of the antiform and synform built by the bedding. (For interpretation of the references to color in this figure legend, the reader is referred to the web version of this article.)

tension of the magma with, in cases, a rotational component that results in oblate spheroidal shapes (Macdonald, 1972; Fisher and Schmincke, 1984; Bates and Jackson, 1987). For the specific case of cannonball, spheroidal composite bombs or accretionary bombs, most of the authors think that they are produced by the repeated eruption and falling back of the particles in the vent (i.e. Schmincke, 1977; Heiken, 1978; Bednarz 1982; Bednarz and Schmincke, 1990; Rosseel et al., 2006; Sottili et al., 2009; 2010). Other authors, however, propose a model assuming fluidal clasts sintering, either by coalescence or agglutination, and welding (formation and solidification) of constituent pyroclasts inside or within the vent/eruption column prior to extrusion or bomb accumulation (Araña and López, 1974; Fisher and Schmincke, 1984; Carracedo Sánchez et al., 2009).

Young cones sometimes display a basal ring made of large bombs that rolled down the slope without breaking (Francis, 1973; McGetchin et al., 1974; Heiken, 1978). Francis (1973) concluded that the spherical shape of many of the bombs at Pacaya volcano (Guatemala) was due to mechanical attrition during their descent of the flank of the cone, and not by processes acting within the volcanic vent or during the first flight of the bomb above the vent. However, the short note of Francis does not have photos or sketches of the bombs, and he also does not describe the deposits associated with minor explosions in the summit crater.

3. Methodology

Fieldwork focused on two existing quarries (Figs. 2 and 3); including detailed lithologic description of the deposits, considering grading, sorting, thickness and description of fragment characteristics (percentages, types). Measurements of the three dimensions of 250 juvenile fragments were made with a vernier caliper, mostly from cannonball bombs but also from other types, collected selectively along all exposed extraction terraces. Structural analyses were also made of joints and faults, regarding type, strike and dip, displacement and frequency. A few bulk deposit samples were collected from lower,

middle and upper portions of selected layers at each sequence from looser portions of the deposit for grain size analysis.

Density measurements of single juvenile fragments were carried out by comparing weights in air and water of clasts wrapped in wax film, following Houghton and Wilson (1989).

Thirteen stratigraphically-controlled samples of juvenile fragments were collected for chemical analysis from the center of the cone to the edge. The XRF and ICP-MS analyses were conducted at Michigan State University following protocols described in Hannah et al. (2000). Electron microprobe analyses were completed at Indiana University, Bloomington on a Cameca SX50, with 15 kV accelerating voltage. The feldspars were probed at 10 nA and a 10 μm beam and the remaining phenocrysts at a 20 nA and 1–2 μm beam size. Chemical diagrams and modeling were carried out with the IGPET-MIXING 2007 program, using least squares regression calculations after Bryan et al. (1969) of major elements from glass and mineral compositions. The viscosity of the magma was calculated using the KWare Magma software (Wohletz, 1999), which uses magma composition, percent and size of crystals as well as estimated water content and temperature.

4. The Cerro Chopo cone

Cerro Chopo (also known as Anunciación, Coronación or Asunción) is a basaltic pyroclastic cone located about 6 km north of the city of Cañas, in northern Costa Rica, and ~25 km trenchward of the northwestern Costa Rican volcanic front (Cordillera de Guanacaste, Fig. 1). The isolated cone is asymmetric, 1670 m long, 810 m wide and 100–185 m high and overlies the 1–2 Ma Monteverde andesitic lavas that lie on the mainly 2–4 Ma Bagaces ignimbritic plateau (Fig. 1). Cerro Chopo forms a N80°W trend with Corobicí (also known as Tierras Morenas) monogenetic cone, located ~14 km NW from Cerro Chopo, and with two isolated basic dyke exposures (Chiesa et al., 1994).

Ramírez and Umaña (1977) and Mora (1977) made the first geological maps and volcanological descriptions. General geochemical

aspects were treated by Tournon (1984) and Chiesa et al. (1994), and its spectacular reverse grading and spherical fragments are also briefly referred by Francis and Oppenheimer (2004).

The Cerro Chopo cone has been extensively quarried since 1954, nowadays consisting of two main quarries: a municipal one to the NW and a private one to the west (Fig. 3). The quarry walls are very steep (55–65°) and the excavation was carried out mostly where the material was relatively loose, principally on three terraces. The total quarried area extends as much as 60 m deep into the volcano, exposing a wall of over 500 m long that is cut by numerous normal faults, permitting a detailed study of the stratigraphy of the deposits (at least 150 m thick) and structure of the volcano. The eastern and western walls of the quarry give excellent exposures through the outer wall of the cone. There is no dating yet for the Cerro Chopo deposits, but their well-preserved morphology, thin superficial soil and slightly weathered tephra, suggest an Upper Quaternary age, probable Late Pleistocene (Mora, 1977; Ramírez and Umaña, 1977).

4.1. Edifice morphology and volume

Most scoria cones are cone-shaped due to the accumulation of cinders and debris around circular vents, but Cerro Chopo is elongated in a NE-SW direction with a length of ca. 1700 m and 850 m wide (Fig. 2). Such morphology has been interpreted as indicating a predominant S70°W wind trend and/or that the eruption occurred along a fissure (Mora, 1977; Ramírez and Umaña, 1977). The lava flows located at the northern and eastern portions of the cone were

erupted from the base, extending about 2.5 km long and reaching a thickness of about 10–15 m (Fig. 2). The volcano is not strongly dissected and its slopes are covered with tropical dry forest. The position of the vent is not clearly defined, but Ramírez and Umaña (1977) and particularly Mora (1977) suggested one near the summit of the cone based on morphology, periclinal structure, changes in degree of welding and grain size (see Fig. 2).

The minimum total volume of tephra was estimated as 0.09 km³, based on the topography and morphology of the edifice and of the lava flows as 0.14 km³. Together, they yield a DRE volume of 0.20 km³ and a volume ratio between the scoria cone and associated lava flows of 1:2.

4.2. Juvenile and accidental clasts and morphologies

The magmatic fragments consist predominantly of low vesicular lapilli to bomb-sized particles and minor ash. Four morphological end-members can be distinguished among Cerro Chopo's juvenile ejecta (Fig. 4): (1) breadcrusted; (2) cannonball; (3) cylindrical; and (4) subangular broken clasts, which are fragments of the other types. All of them exhibit different morphologies and degrees of vesicularity, but are still in the range of incipiently to poorly vesicular (5–40%) fragments, according to the classification of Houghton and Wilson (1989). Accidental lithic fragments are only found at the lowermost exposed portion of the western section, related to phreatomagmatic deposits, and are mainly andesitic lavas. The rest of the cone instead lacks completely of accidental lithics.

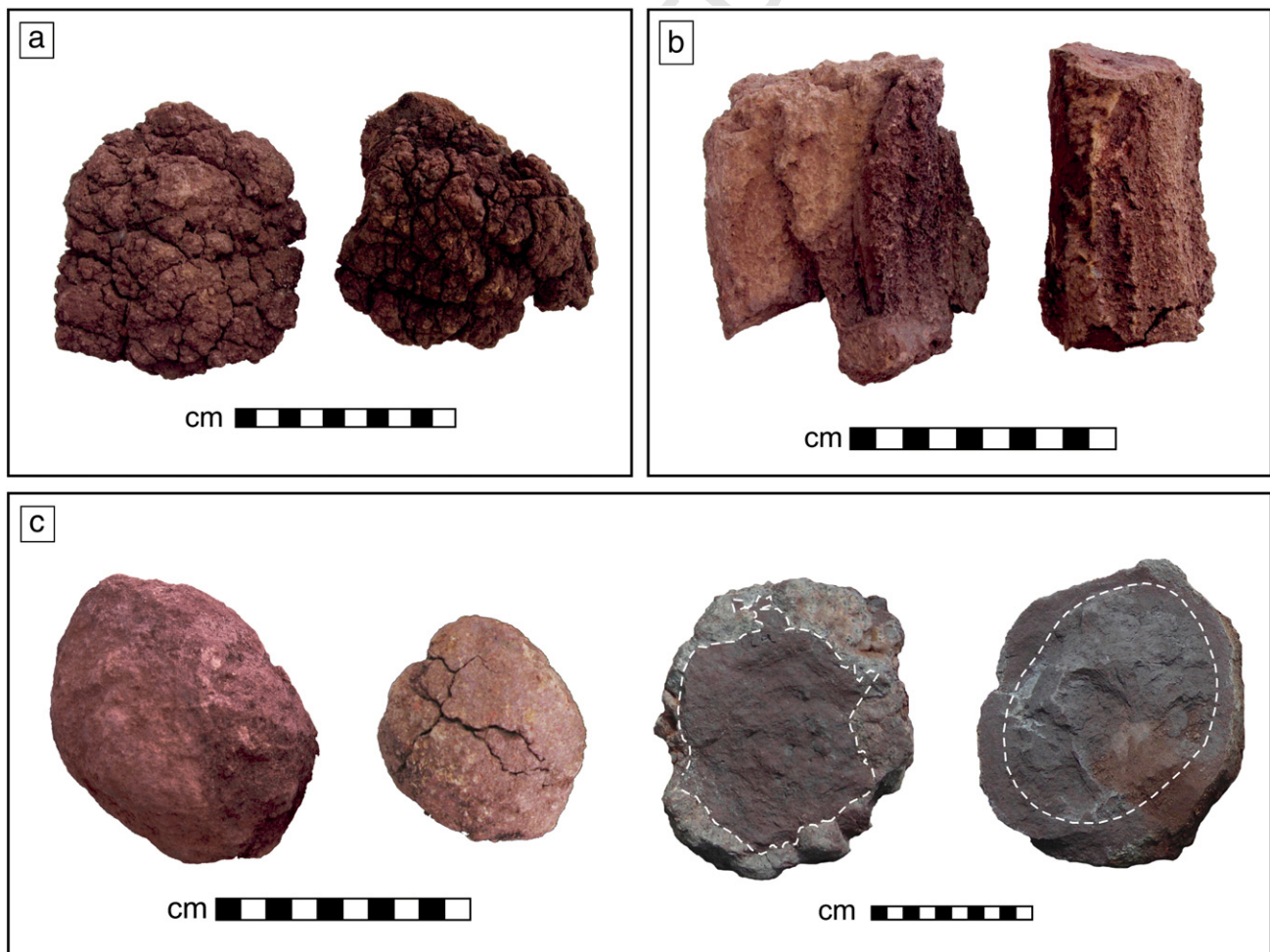


Fig. 4. Major types of juvenile fragments of the Cerro Chopo cone: a. breadcrusted bombs, b. cylindric bombs and c. cannonball bombs. The cannonball can be ellipsoidal or spherical in shape, some with incipient to well breadcrusted structure, and their internal structure shows frequently a rind. No pictures from broken clasts are shown.

The breadcrusted bombs are the most abundant type at Cerro Chopo, and even some cannonball, cylindrical or fragmented bombs can show partially breadcrust features. They have chilled and thin and shallow cracked surfaces; a few larger vesicles (up to 5×2 cm) are restricted to the core of the clasts.

The cannonball bombs and lapilli are also very common. We refer here as cannonball fragments to dense, poorly vesicular clasts with a nearly spherical shape and relative smooth surface, also named spherical or ellipsoidal bombs in the literature as well. They have a crust and a core and can be divided into two groups: the most common variety has round smooth surfaces and poorly vesicular cores (vesicles 5 mm in diameter) or a uniform lava-like rind surface. The other type has an irregular surface and in their interior it is possible to recognize lapillistone cores or cylindrical-like bombs; lapilli can also be impressed into the outer rind surfaces or form rind surfaces themselves with fragments up to 2.5 cm in diameter. It is also common to find cannonball bombs with a breadcrust surface (see photo in Figs. 4, 5 and 6).

Cylindrical-shaped bombs are relatively abundant at the eastern sequence, though very rare at the western sequence. They are the least

abundant type of juvenile fragments with moderate vesicular interiors (size 5×0.4 cm) and thin non- to poorly vesicular rims cut by echelon tension cracks. Many of the large clasts broke on landing and the resulting rare fragmented bombs (blocks) are angular to subrounded, non-vesicular to microvesicular, completely or not oxidized at all.

We obtained geometric shape parameters based on the length of the three main axes (A the longest, B intermediate and C the smallest) from 250 bombs and lapilli. The diagram from Zingg (1935) shows that many of the cannonball fragments have an ideal spherical shape, with the three axes of the same or very similar length and, therefore, yielding a Krumbein (1941) roundness value equal to 1 (dashed curved lines in Fig. 6). Overall, the roundness for the cannonball clasts ranges from 0.6 to 1.0, the smallest values representing a more ellipsoidal shape. The cylindrical bombs exhibit the lower roundness values (between 0.4 and 0.8) from Chopo, whereas the typical breadcrusted bombs represent different types of geometries. In addition, cylindrical bombs occupy all fields of shape type, an indication that these bombs do not exhibit a well developed defined shape, but a transition between smooth cannonball (some with incipient

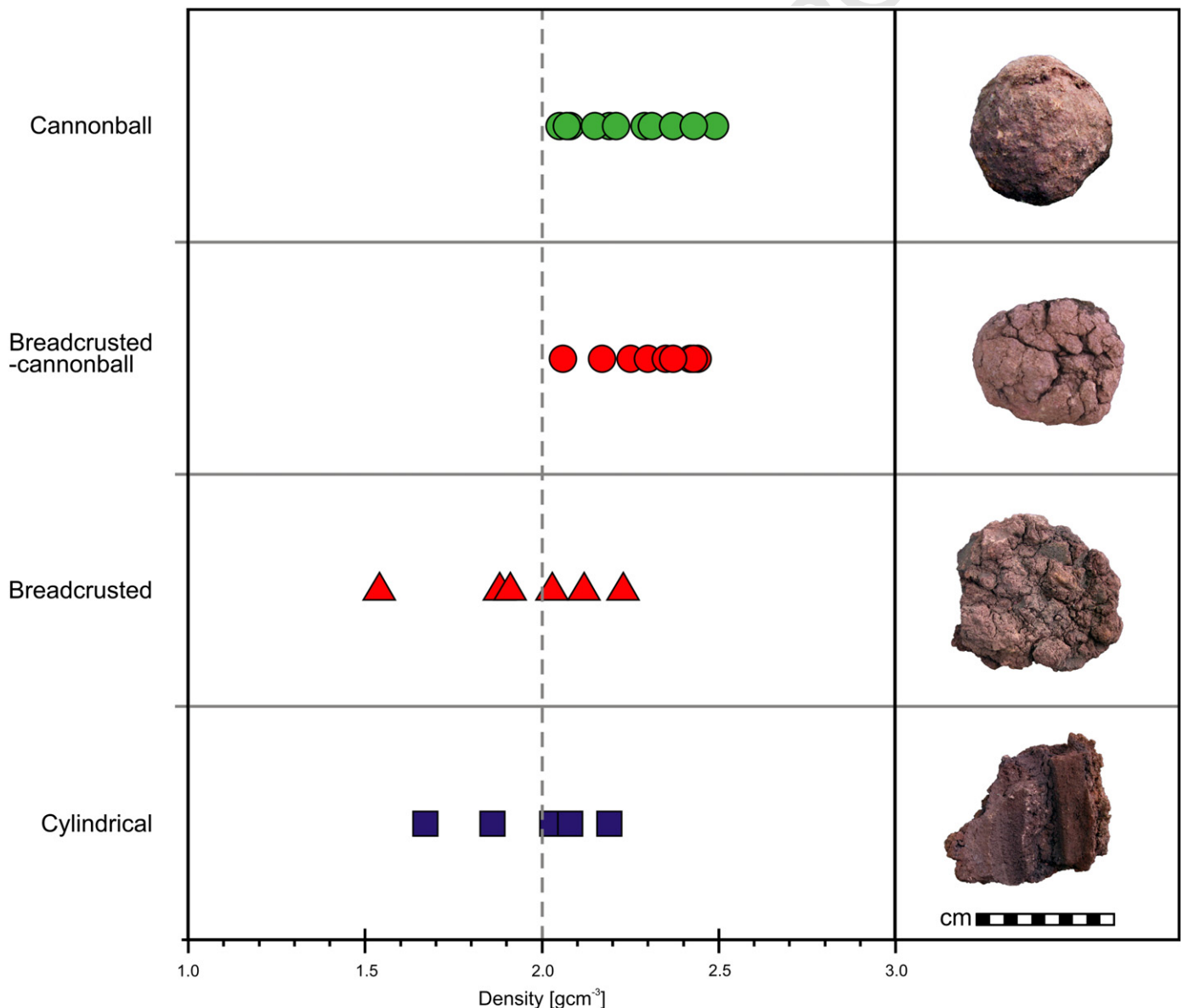


Fig. 5. Density variations of the main clast types. Note that cannonball bombs with breadcrusted structure exhibit a density higher than 2 g/cm^3 , same as typical cannonball fragments.

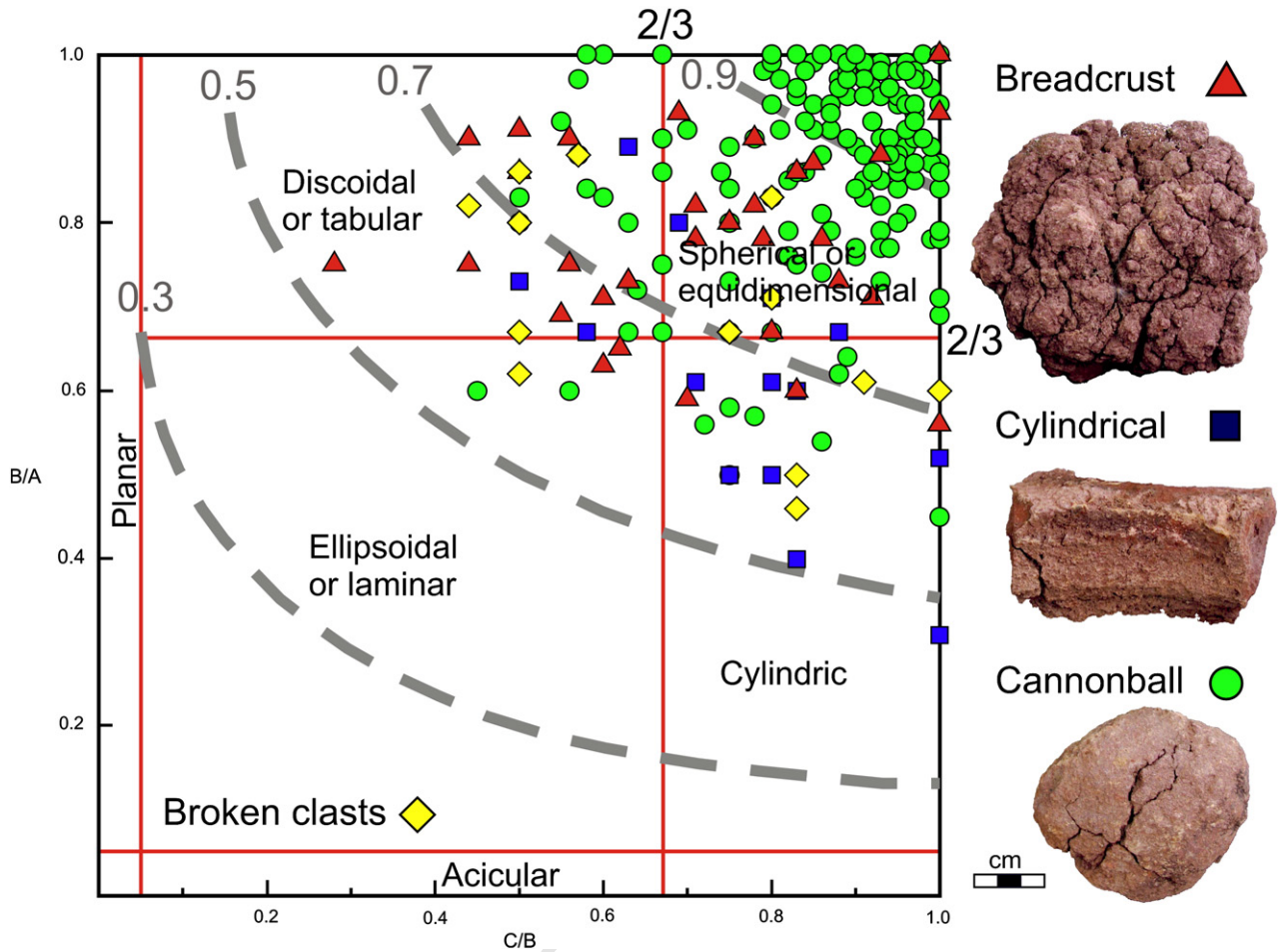


Fig. 6. Diagram B/A versus C/B, where A is the longest axis, B the intermediate and C the smallest, of the different types of volcanic bombs and their relationship with sphericity of Krumbein (1941) indicated by the curved lines (modified after Zingg, 1935 and Brewer, 1964). No pictures from broken clasts are shown.

breadcrust structure) and typical breadcrusted types with a more irregular shape.

We also calculated geometric parameters like the roundness index, calculated as $(A + B)/2C$, and the smooth flatness index calculated as $(A + B + C)/3$. The roundness indices of the cannonball bombs vary between 1.00 and 2.40, similar to that of the cylindrical bombs but much less than those of the breadcrusted. The smooth flatness index is similar to all the main types except the broken ones corresponding with the field observations (Table 1).

In general, the low vesicularity of the juvenile fragments is reflected in high bulk densities (Table 1). Vesicular portions in bombs from Cerro Chopo are normally restricted to the central portions of the clast. When comparing the density of the bomb types, it is clear that the cannonball and cannonball fragments with breadcrust structure have a higher density ($>2 \text{ g/cm}^3$) than the other types (Fig. 5). Similar

densities to those of the cannonball bombs are observed in spherical to ellipsoidal lapilli at Herchenberg cone; values clearly higher than average densities of vesicular bomb populations (Bednarz and Schmincke, 1990). The ranges of density and vesicularity of the Chopo cylindrical bombs are similar to those of the breadcrust clasts.

Grain size analyses in order to quantify sorting and changes in grain size, were carried out in samples at lower, middle and upper portions of selected layers. The analyses show a unimodal distribution with over 90% of the components larger than 1 mm, and practically no fine-grained fraction. The lower part of the beds is finer-grained, with largest particles being ~1 cm in diameter, whereas the middle and upper parts have lapilli clasts larger than 4 cm. Collected samples show a general increase in the mean grain size (from -2 to -4 phi) and a decrease in the sorting upwards in the stratigraphy, from well-sorted at the lower part to moderately sorted at the top.

4.3. Petrographic and geochemical aspects

Cerro Chopo tephrae are quartz normative, high-alumina olivine tholeiitic basalts, which contain large (up to 6 mm; usually 1 mm in diameter) euhedral olivine phenocrysts (~8 vol.%, Fo_{67-69}) with inclusions of chromium spinel. Plagioclase phenocrysts are rare (<1 vol.%), euhedral with patchy zones (An_{49-83}), and oriented inclusions. Augite phenocrysts are euhedral up to 2 mm in diameter (2.5 vol.%, $\text{Wo}_{70-84} \text{En}_{13-19} \text{Fs}_{2-10}$). The Fe-Ti oxide phenocrysts and microphenocrysts are magnetite. The groundmass ranges from interstitial to microlitic, consists mainly of plagioclase, clinopyroxene, magnetite, and rare olivine and apatite (Fig. 7).

Table 1
Parameters for the different juvenile clasts from Cerro Chopo. Given values are minimum, maximum and average (in parenthesis).

Parameter	Breadcrust	Cannonball	Cylindrical	Broken
Density g/cm^3	1.54–2.23	2.05–2.49	1.67–2.19	1.54–2.37
Vesicularity %	~15–40%	~5–20%	~15–35%	~5–40
Roundness index	1.00–4.20 (1.64)	1.00–2.40 (1.50)	1.50–2.37 (1.84)	1.37–2.62 (1.83)
Smooth flatness index	5.00–14.33 (9.37)	2.50–15.66 (7.00)	3.16–14.33 (7.25)	3.66–8.33 (5.56)

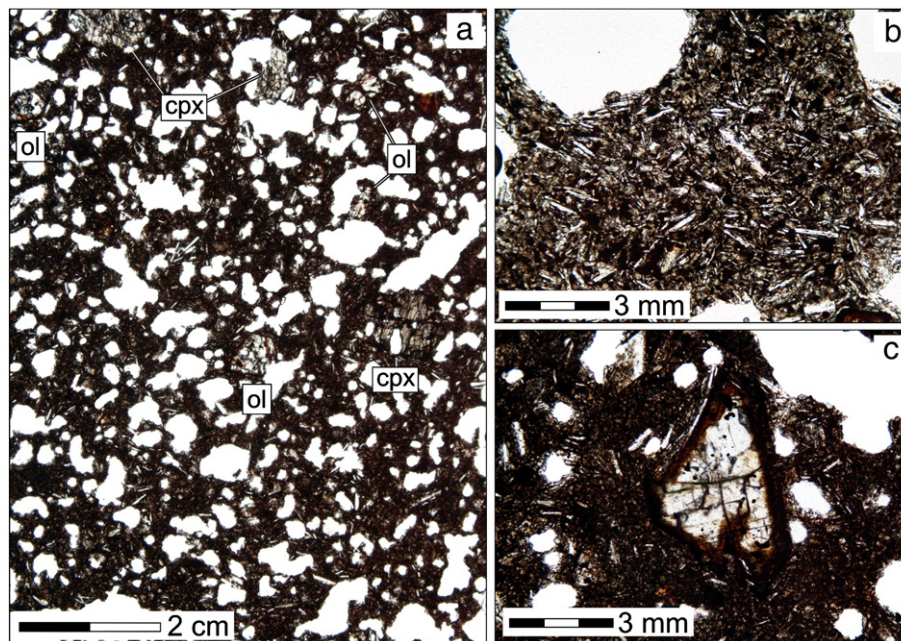


Fig. 7. Microphotographs of the Cerro Chopo rocks: a. poorly vesicular (30%) bomb with olivine and pyroxene phenocrysts; b. detail of the matrix, rich in plagioclase, pyroxene and magnetite microliths; and c. partially oxidized olivine phenocryst.

Major element trends are illustrated in Fig. 8 and bulk rock compositions are given in Table 2. Overall the major oxide composition is relatively constant. There is very little variation in silica (47.5–48.7 wt.% SiO₂), whereas MgO varies from 5.3 to 7.2 wt.%; FeO slightly increases and MgO decreases with distance outwards from the center of the cone. The decrease in MgO and Ni (41–103 ppm) is small, which is consistent with a small amount of olivine fractionation (see later), and there is no Eu anomaly consistent with the lack of plagioclase fractionation. The pattern of Cerro Chopo samples in a multi-element spider diagram in Fig. 9, normalized to primitive mantle (Sun and McDonough, 1989), is similar to the pattern of HAOTs lavas (sensu Hart et al., 1984) associated with an island arc environment (Bacon, 1990), with enrichments in Sr and Ba relative to Rb, K, and depletions of Nb and Ti.

4.4. Stratigraphy

The cone is relatively homogeneous, consisting of well-bedded, moderately to well-sorted deposits of intensely oxidized, unconsolidated, reddish scoria lapilli and bombs that become finer towards the top (lapilli to ash fractions). A difference is marked by the deposits cropping out at the basal portion of the western sequence, which show no oxidation. We distinguish between eastern and western sections along the quarry wall at Chopo, according to the grain size and structural variations (Figs. 3 and 10). The western studied section (~150 m thick) is composed of well-bedded deposits of ash to lapilli layers with pinch-and-swell structures and a small bomb population. The eastern one is coarser-grained (lapilli to bombs) and is cut by numerous faults, obscuring the bedding. The maximum tephra thickness is estimated in at least 300 m. The loose nature of the deposits and the working at the quarry, contribute to the growth of basal talus fan deposits.

4.4.1. East section descriptions

The eastern part of the quarry is ~140 m thick and is dominated by coarse-grained deposits composed of well-sorted, poorly to moderately vesicular lapilli and bombs. Crude and well-defined bedding consists of grain size changes from fine lapilli to bombs (Fig. 10). Individual layer boundaries are generally non-erosional and plane-parallel with relatively good lateral continuity over several meters or more but locally there are thick disorganized volcanic breccias. The

beds are as thick as 4 m and very homogeneous, composed mostly of cannonball (~60 vol.%), breadcrust and broken bomb fragments with rare (<3 vol.%) cylindrical lapilli-bomb size fragments. The bombs are up to 65 cm in diameter and are also found as flattened, highly vesicular slabs up to 2.4 m long by 10–40 cm thick with plastic deformation (Fig. 11b). The dominant grain size ranges from 0.1 to 5 cm at the base to bomb size clasts at the top. Some beds exhibit a symmetric grading (reverse to normal), but the dominant reversely graded layers are 15–40 cm thick. Welding is common near the vent suggested by Mora (1977; Figs. 2, 11c) and the deposits typically consist of alternating slightly welded beds (lapillistones, bomb breccias) to densely welded layers where clast boundaries are obscured, and therefore the grading is not evident. The outer wall beds dip between 11 and 34° outward from the vent. Dipping angles larger than 34° are too steep for primary deposits, and these dips resulted from abundant faults at the lower- and westernmost portions of the eastern sequence that tilted the layers.

At the lower part of the sequence the faults are filled with fine consolidated ash and the faults strongly affect the bedding angles, increasing them to up to 50°–80°, simulating unconformities. In general, the faults in the middle and upper part of the eastern section are poorly developed or not easily recognized because of their small displacement in poorly-stratified and coarse-grained deposits.

4.4.2. West section descriptions

A recent excavation front of the quarry on the west margin of the volcano exposed the lowermost part of the cone. The deposit consists entirely of about 8-m-thick, weakly bedded moderately vesicular brownish lapilli layers, rare bombs and abundant andesitic accidental lithic fragments with different textures (up to 30 cm in size; Figs. 2 and 11a). These deposits are volumetrically restricted to only one part of the sequence (Fig. 2).

The western sequence consists of at least 150 m thick of well-bedded deposits of well- to moderately-sorted, poorly to moderately vesicular lapilli and ash fragments with some bombs. The bombs are up to 40 cm in diameter; cylindrical bombs are very rare. Elongated bombs and lapilli within beds are rarely imbricate. Individual beds are as thick as 1.5 m; single, inversely graded layers are commonly about 15–50 cm thick. The light-colored ash layers are a distinctive feature of each main

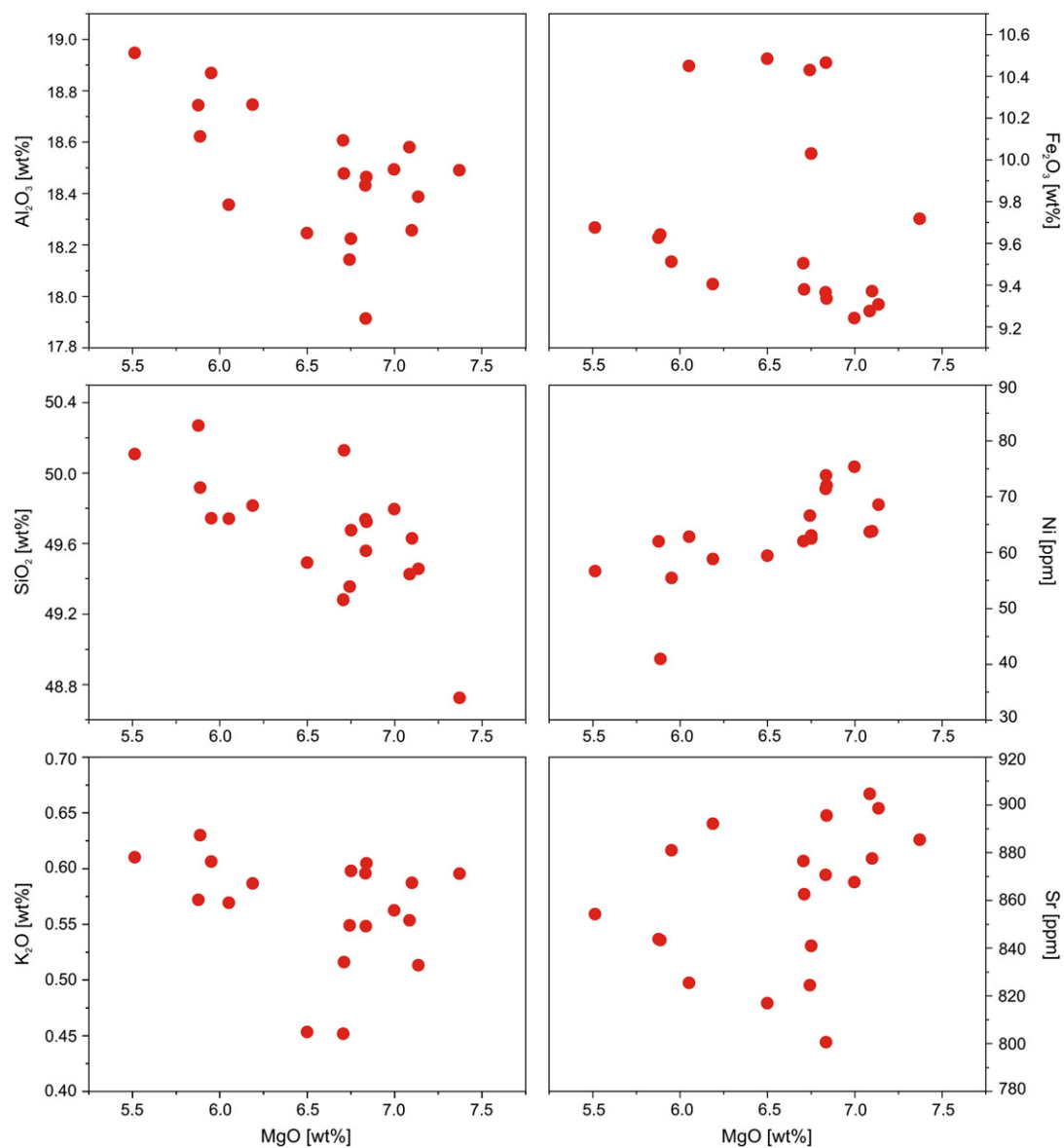


Fig. 8. Major and trace element compositions of the Cerro Chopo tephras.

460 layer, and form the base of the inversely-graded part of certain beds. The
 461 fine layers are well-laminated, not always continuous (lateral discontinuity),
 462 with floating bombs but without bomb sag structures. Some of the beds are
 463 composite, and lamination is marked by the presence of coarse ash and fine
 464 lapilli, laterally with variable thickness of coarse lapilli/bomb lenses or even
 465 as bomb or lapilli swarms or observable as trains of well-sorted coarse
 466 material. The upper part of the sequence is locally dominated by yellowish-brownish
 467 lapilli-tuffs (Fig. 11d, e, f). The outer wall beds dip outward from the vent at
 468 angles ranging from 22° to 35°. Also, there is a lateral increase of the size and
 469 content of coarse tephra along the dipping down slopes.

471 4.5. Structure

472 The bedding angles form NNW-SSE to N-S synform and antiform
 473 primary (depositional) structures (Fig. 3). The cone is cut by abundant
 474 faults with differences in the degree of preservation and type of
 475 movement. The faults are better developed and easy to recognize on the
 476 west because the deposits are finer grained and well-bedded. Some
 477 secondary white minerals (may be zeolites and/or amorphous silica)
 478 have precipitated on several fault planes, due to surface weathering or

479 precipitated by fumarolic steam from rainwater percolating through the
 480 still hot cone. We studied 115 small-scale faults in Cerro Chopo and
 481 found 82% show strike directions of N 30°–60° E and 18% are N–S, these
 482 are located near the proposed vent. Most of the faults dip 30°–60° to the
 483 southwest, and east or less frequently to the west. The majority of the
 484 faults have an apparent normal component and the presence of a lateral
 485 component could not be determined because of the lack of preserved
 486 slickensides in soft tephra. We could recognize a dextral strike-slip
 487 displacement in only a few faults, which due to the dipping of the
 488 layers laterally produced a reverse-like movement. The maximum observed
 489 displacement is approximately 4 m, but it usually was a few
 490 centimeters. There are also beds showing bending flexure and in other
 491 cases the displacement is only at the base, suggesting some volcano-
 492 tectonic control.

493 5. Mode of growth of the pyroclastic cone

494 5.1. The nature of the eruption style

495 The characteristics of the deposits at Cerro Chopo permit inter-
 496 pretation of three main styles of volcanic activity, which contributed

Table 2
Bulk rock compositions of stratigraphic samples from Cerro Chopo.

Sample	1	2	3	3.1	4	4.1	5	6	7	8	9	10	11	12	13
SiO ₂	48.20	48.17	48.41	48.17	47.46	49.01	48.40	48.50	48.33	47.99	48.56	48.45	48.39	48.68	48.33
Al ₂ O ₃	18.12	17.91	17.94	17.72	18.01	17.98	18.36	18.01	18.02	18.12	17.90	18.32	18.21	18.08	18.03
FeO	9.05	9.07	9.12	9.10	9.47	9.90	9.26	9.11	9.26	9.26	9.09	9.36	9.14	9.04	9.34
MgO	6.91	6.95	6.65	6.89	7.18	6.66	5.79	6.67	5.65	6.53	6.50	5.33	6.01	6.84	5.70
CaO	11.06	11.17	10.99	10.98	11.05	11.08	11.18	11.04	10.90	11.28	10.85	11.07	11.21	11.04	11.06
Na ₂ O	2.40	2.38	2.37	2.38	2.38	2.15	2.46	2.42	2.18	2.43	2.23	2.26	2.35	2.31	2.46
K ₂ O	0.54	0.50	0.58	0.57	0.58	0.59	0.59	0.59	0.55	0.44	0.50	0.59	0.57	0.55	0.61
TiO ₂	0.82	0.81	0.81	0.81	0.82	0.85	0.83	0.83	0.82	0.84	0.81	0.84	0.83	0.82	0.84
P ₂ O ₅	0.24	0.26	0.28	0.26	0.26	0.27	0.25	0.19	0.26	0.31	0.26	0.29	0.25	0.23	0.27
MnO	0.18	0.18	0.18	0.18	0.19	0.17	0.18	0.18	0.17	0.18	0.17	0.18	0.18	0.17	0.18
Cr	180	166	186	214	1157	179	183	187	191	188	214	186	197	188	199
Ni	64	69	71	64	163	63	55	72	62	62	103	57	59	75	41
Cu	119	118	100	115	122	169	138	119	103	134	130	109	113	112	130
Zn	51	50	51	79	56	78	94	65	70	71	82	146	84	107	82
Rb	16	7	8	7	14	11	8	13	12	15	23	12	19	20	5
Sr	905	899	871	878	885	841	881	896	844	876	863	854	892	868	843
Y	19	19	19	20	12	16	13	10	12	16	16	18	17	15	23
Zr	75	71	66	74	71	73	76	76	76	79	73	75	81	71	77
Nb	2	4	ND	ND	ND	ND	3	2	8	8	4	1	3	ND	ND
La	ND	ND	10	23	ND	10	3	30	12	21	17	24	14	15	13
Ba	388	508	516	410	480	436	489	472	543	487	389	447	445	404	427
Total	97.52	97.40	97.33	97.06	97.40	98.66	97.30	97.54	96.14	97.38	96.87	96.69	97.14	97.76	96.82

to the formation of the cone: a) phreatomagmatic activity related to the formation of a tuff ring/cone, b) Strombolian activity forming the main pyroclastic cone, and c) lateral lava flows.

The local phreatomagmatic sequence is overlain by the main products of Cerro Chopo, which have a “dry” magmatic signature, typical of Strombolian deposits generated by moderate accumulation rate of warm to hot pyroclastic deposits (e.g., Walker and Croasdale, 1972; Kokelaar, 1986; Houghton and Wilson, 1989). This signature includes: coarse grained (indicative of a low degree of fragmentation), well-sorted, well-bedded, lithic-free, cylindrical bombs, agglomerate breccias, usually reddened by stream oxidation and a wide vesicularity range in the coarse-grained deposits. Juvenile lapilli show small vesicles, whereas the bombs have a few relatively larger vesicles at the core of the fragment, indicating that vesiculation continued after fragmentation in a low viscosity basaltic magma. Locally, some degree of welding (agglomerates, and even clastogenic lavas or agglutinates) is indicative of fluid fragments and/or a higher rate of accumulation of hot pyroclasts.

However, two aspects are not totally consistent with a magmatic origin: a) the high density and low vesicularity (5–40%) of the juvenile

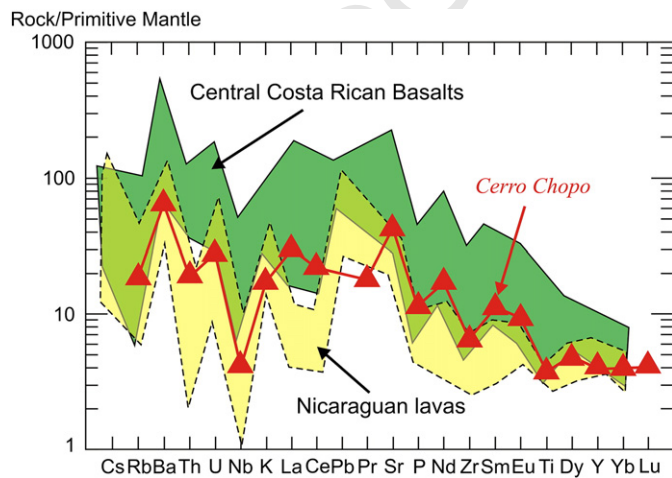


Fig. 9. Multi-element compositions, normalized to primitive mantle by Sun and McDonough (1989), of an average of Cerro Chopo rocks compared with those of lavas from Central Costa Rica and Nicaragua.

clasts, in contrast with the vesicularity of ~70–80% of magmatic deposits elsewhere regardless of magma viscosity (Houghton and Wilson, 1989; Mangan and Cashman, 1996), and b) the abundance of breadcrust clasts, which is similar to deposits related to Vulcanian eruptions (see Wright et al., 2007). In the absence of clear evidence for involvement of abundant external water (e.g. fine ash, vesicular tuffs, accretionary lapilli, mud cracks, quenched glassy juvenile blocks, etc.), the deposits can be only comparable to products from magmatic (=dry) Strombolian activity. Thus, the limited variations in vesicularity could be explained in this case by differences in residence times and degassing stage of the different magma pulses (Blackburn et al., 1976; Heiken, 1978; Houghton and Hackett, 1984; Lautze and Houghton, 2005). The eruption probably resulted from cyclical declining supply of fresh gas-rich magma, leading to stagnation and perhaps the formation of a lava pool, and decreasing vigor of the explosions. Indeed, the presence of some large slabs could suggest the existence of lava ponds or maybe even a lava pool. The low viscosity of the Chopo magma, calculated in $5-9 \times 10^2$ Pa s –typical of basaltic fluid magma (i.e. Cas and Wright, 1987)–, favored also these conditions.

Other process that generally produces juvenile clasts with a wide range in vesicularity, including low vesiculated dense bombs, is the recycling through the vent and the flight times (= cooling time). This means the fragments fell back into the crater (ballistic and/or grain avalanches) and are re-ejected into the air, and so on, until they finally land on the flanks (i.e. Guilbaud et al., 2009). We propose the eruption was a mixture of less degassed magma and degassed magma that had a long-residence time at the vent, ponding in the conduit and leading to open vent degassing and crystallization of the matrix.

5.2. Origin of the reverse grading

Alternating coarser- and finer-grained reverse beds is a very distinctive feature in Cerro Chopo in all the exposed quarry walls from the base to the top. The origin of reverse grading in fallout deposits has been ascribed to different causes (see Introduction), but due to the exclusive subaerial volcanism during cone formation only a few of them are plausible. These are related to eruptive processes, like would be changing conditions at the vent or an increase in initial gas velocity and/or eruption column density, a decrease in explosivity or a decrease in the degree of fragmentation as well.

Another mechanism could be the rolling of large clasts over smaller clasts on the surface of a steep slope by self-sieving of the very

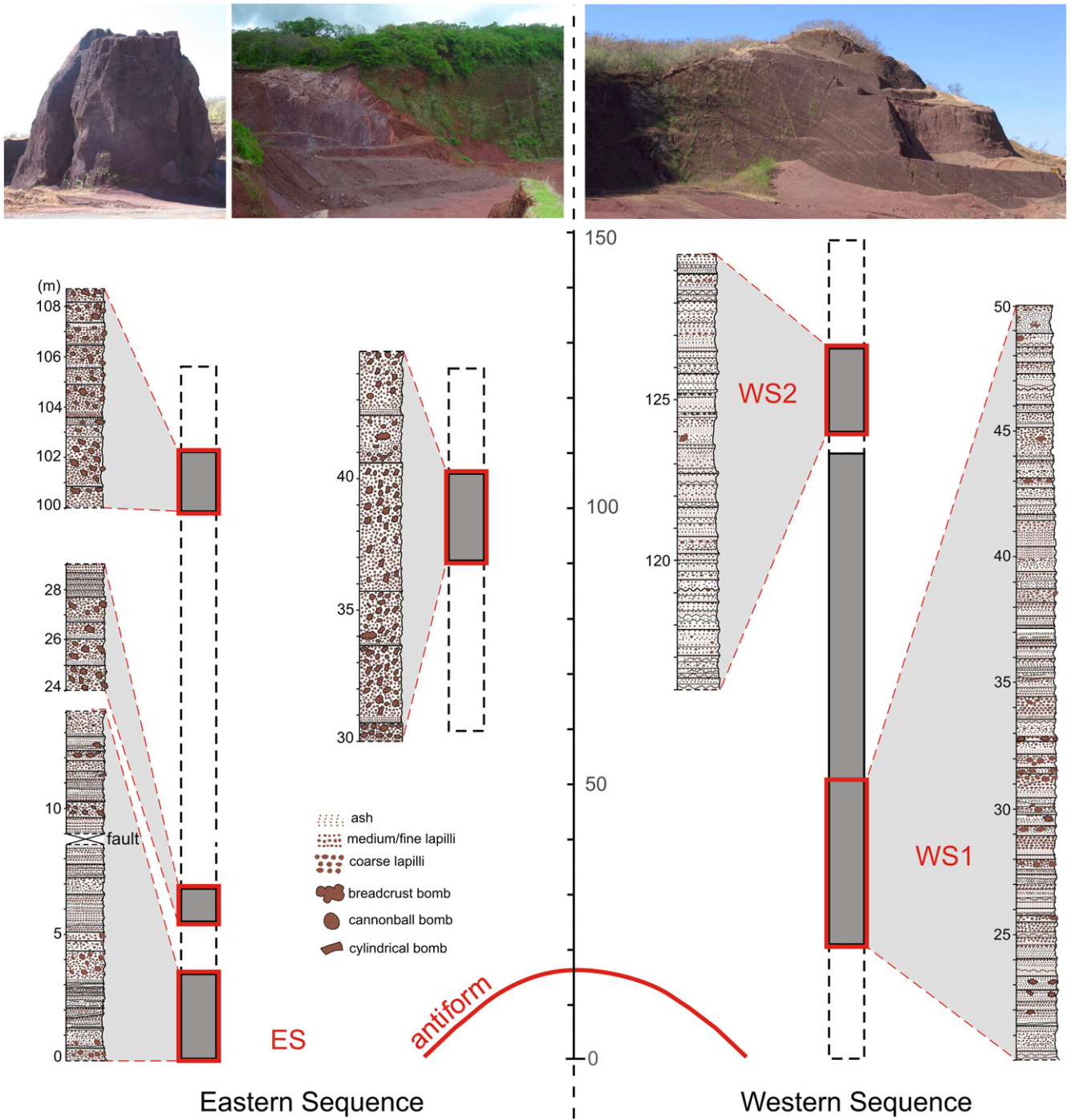


Fig. 10. Stratigraphic profiles of the eastern and western sequences of the studied area shown in Figs. 2 and 3. Both profiles are located at opposite sides of the antiform, the eastern sequence is coarser grained than the western sequence, represented by a higher bomb population which also suggests nearer vent facies. Gray parts represent studied parts of the stratigraphy.

557 loose tephra upon sliding, so that it exceeds the repose angle and
 558 moves down slope (Fisher and Schmincke, 1984; Houghton et al.,
 559 2000). Indications of this are the lack of ash matrix, the common
 560 presence of well-sorted bomb/lapilli layers, and the increase of clast
 561 size toward the margin of the layers. These features have been
 562 interpreted mainly in terms of the grain-flow theory of Bagnold
 563 (1954) as modified grain flows (Sohn et al., 1997). At Cerro Chopo,
 564 actual stability angles of artificial slopes and coluvial or talus fans in
 565 the quarry range from $\sim 31\text{--}34^\circ$, which is the same as the angles of
 566 repose at fresh scoria cones (Cas and Wright, 1987) and correspond
 567 to the dipping angles of the reverse-graded beds. In addition, there are

several beds showing a lateral increase in thickness and size of coarse
 568 clasts down slope (Fig. 11f), and clast imbrications and pinch and
 569 swell features are also noted. These structures are indicative of rolling
 570 to a preferred orientation during down slope transport, and again it
 571 can be attributed to a range of gravity-controlled processes, including
 572 sliding of individual ballistic tephra or of a blanket of accumulating
 573 fragments down the slopes of the cone, as was also observed in
 574 alluvial fan deltas (i.e. Sohn et al., 1997). The gravity-controlled
 575 processes could have been triggered by the impact of large bombs
 576 and/or earthquakes associated with the Strombolian eruption, or
 577 simply the slope exceeding the angle of repose during rapid
 578

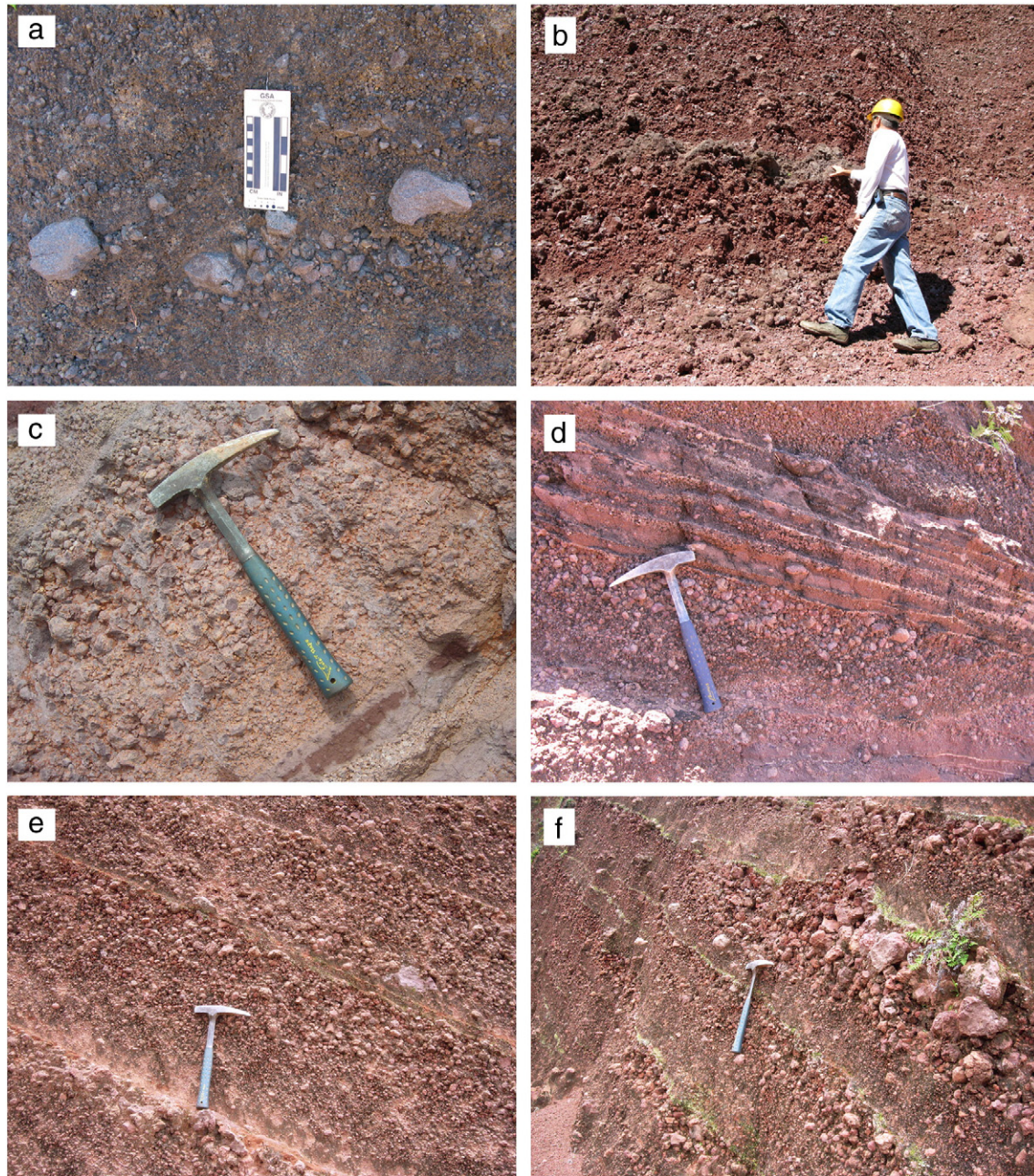


Fig. 11. Various photographs showing the deposits and other features at Cerro Chopo: a. basal lithic-rich phreatomagmatic beds; b. large bomb slab at the eastern sequence near the suggested vent; c. agglomerate at the vent-near facies; d. finer ash beds, abundant mostly at the upper portions of the Western sequence; e. ubiquitous typical reverse grading present at Chopo, and f. coarse-grained lens evidencing down slope rolling of large clasts.

deposition. However, although this is the most accepted model and easy to apply, there is a problem, which is that the reverse grading is present everywhere, including at the top of the exposed cone, very close to the supposed crater, and from the beginning to the end of each layer. Thus, varying explosive conditions at the vent should be considered. Another factor may be lower explosivity and/or less efficient magma fragmentation, generating large juvenile clasts.

5.3. Origin of the different juvenile fragment types

The morphological division of the juvenile clasts suggested here is only to separate end-members from a continuous spectra, since there are several fragments which show features from two groups, e.g. well-shaped cylindrical and cannonball bombs but with breadcrust rinds. Almost each bed at Cerro Chopo contains breadcrusted, cannonball and

broken bombs with less frequent cylindrical clasts, thus suggesting that the different types of ejecta followed similar eruptive paths.

The cylindrical bombs may have formed, as proposed by Macdonald (1973), by fluid magma ejected as both long irregular strings and discrete blebs of liquid. Breadcrust bombs can form via three distinct mechanisms in a relatively degassed magma with a moderate viscosity that undergoes open-degassing system (see Wright et al., 2007): (1) interior expansion after outer rind formation (Darwin, 1845; Rittmann, 1960); (2) thermal contraction of the rind; and (3) stresses applied during the impact (Wright et al., 2007). All three mechanisms likely contributed in different proportions to the surface morphology of the cracked bombs and lapilli found at Cerro Chopo. The broken bombs likely formed due to impact with other clasts or upon landing.

The cannonball bombs and lapilli (several also with breadcrusted surface and very abundant at Chopo) are interpreted to represent

607 more complex origins than the other clast types. Most of these
 608 spherical shaped clasts present a rim with smooth surfaces, easily
 609 distinguished from the internal core, whereas in other cases they
 610 exhibit an armored lapilli structure. It is likely that these fragments
 611 originated when degassed magma ejected as separate blebs that
 612 tended to be pulled into spheres of pasty lava, helped by mechanical
 613 rounding processes while traveling at high speed down the slopes, as
 614 suggested by Francis (1973). Part of the armored-type of cannonball
 615 clasts, those with a lapilli rind, could be interpreted to have formed by
 616 accretion of hot fragments during rolling. Evidence of rolling includes
 617 the armoring with talus hot fragments, the reverse grading and other
 618 evidences of transport direction described earlier (i.e. tephra horizons
 619 that pinch out laterally, clast imbrications, high steep slopes). The
 620 ones with uniform lava-like rims may have formed by recycling of
 621 clasts due to falling back in the vent (Bednartz and Schmincke, 1990;
 622 Guilbaud et al., 2009).

623 Parfitt and Wilson (1995) have demonstrated that high magma
 624 ascent rates rather than elevated volatile contents control the
 625 explosivity of basaltic eruptions, producing high ejecta velocities;
 626 the consequent long flight paths cause clasts to lose heat to the
 627 atmosphere and to land as relatively rigid fragments (Wolff and
 628 Sumner, 2000). This scenario could explain the existence of
 629 cannonball clasts usually with no plastic deformation in the west
 630 section. In addition, the wind and the asymmetrical morphology of
 631 the vent played an important role in the sorting, deposition and
 632 cooling of the tephra: fine to medium grained lapilli/ash deposits with
 633 bombs without deformation in the SW part of the cone, and coarse
 634 grained (bomb layers, bomb breccias, agglomerate and agglutinate) in
 635 the NE. The present wind direction (S70–75°W) has the same
 636 asymmetrical orientation of the elongated axis of Cerro Chopo.

637 5.4. Geochemical interpretation

638 As predicted by the lack of significant variation in the concentra-
 639 tion of major and trace elements, fractional crystallization has not
 640 played a major role in differentiation among these samples, being
 641 restricted to less than 5%. The lack of chemical variation and absence
 642 of large plagioclase phenocrysts in Cerro Chopo samples supports the

643 hypothesis that there is no large, shallow level magma chamber
 644 beneath the cone (Hasenaka and Carmichael, 1987). HOAT basalts
 645 have been interpreted to represent a primary magma, generated near
 646 the crust–mantle boundary (Tatsumi et al., 1986).

647 Chopo cone is located in the transition zone between the MORB-
 648 like source for the northern part of the Central American Arc and the
 649 OIB-like source underneath Central Costa Rica (Feigenson and Carr,
 650 1993; Herrstrom et al., 1995). Based on La/Yb ratios, we propose that
 651 Cerro Chopo lavas tap a source similar to the enriched MORB source,
 652 with minor participation from the OIB source. Trace element ratios of
 653 the Cerro Chopo lavas suggest that they originated from a mixed
 654 mantle source that has been variably modified by the subducting slab
 655 (i.e. sediment input).

656 5.5. Comparison of Cerro Chopo with other pyroclastic cones

657 As we mentioned in the Introduction, Chopo is not a typical cinder or
 658 scoria cone where highly vesiculated clasts are very frequent. From about
 659 a dozen cones with spherical bombs reported at the moment, only six
 660 cases are well studied (Fig. 12): Rothenberg and Herchenberg cones at
 661 Germany (Bednartz, 1982; Houghton and Schmincke, 1989; Bednartz and
 662 Schmincke, 1990), Pelagatos scoria cone in Mexico City (Guilbaud et al.,
 663 2009), the Rotomahana vent at Tarawera in New Zealand (Rosseel et al.,
 664 2006), Colli Albani volcanic district (Sottili et al., 2009, 2010), and
 665 Cabezo Segura volcano in Spain (Carracedo Sánchez et al., 2009).

666 The deposits from the Rotomahana historical eruption at Tarawera
 667 or from the Colli Albani Volcanic District have abundant cored juvenile
 668 clasts, containing cores of subvolcanic country rock (Rosseel et al.,
 669 2006; Sottili et al., 2009, 2010). Less frequent are these cores in Cabezo
 670 Segura volcano (Spain) but cover a wide spectrum from mantle
 671 xenoliths and xenocrysts, to solidified juvenile rock fragments and
 672 crystals (Carracedo Sánchez et al., 2009). The abundance of lithic cores
 673 in the cored juvenile bombs/lapilli may be due to two main reasons: a)
 674 phreatomagmatic to Strombolian transitional deposits, as reported in
 675 tuff/cinder cones or maar, even diatreme structures (Fisher and
 676 Schmincke, 1984; Rosseel et al., 2006; Carracedo Sánchez et al., 2009;
 677 Sottili et al., 2009, 2010), and b) the very common and well-known
 678 presence of mantle xenoliths in alkali mafic volcanism (i.e. Fisher and

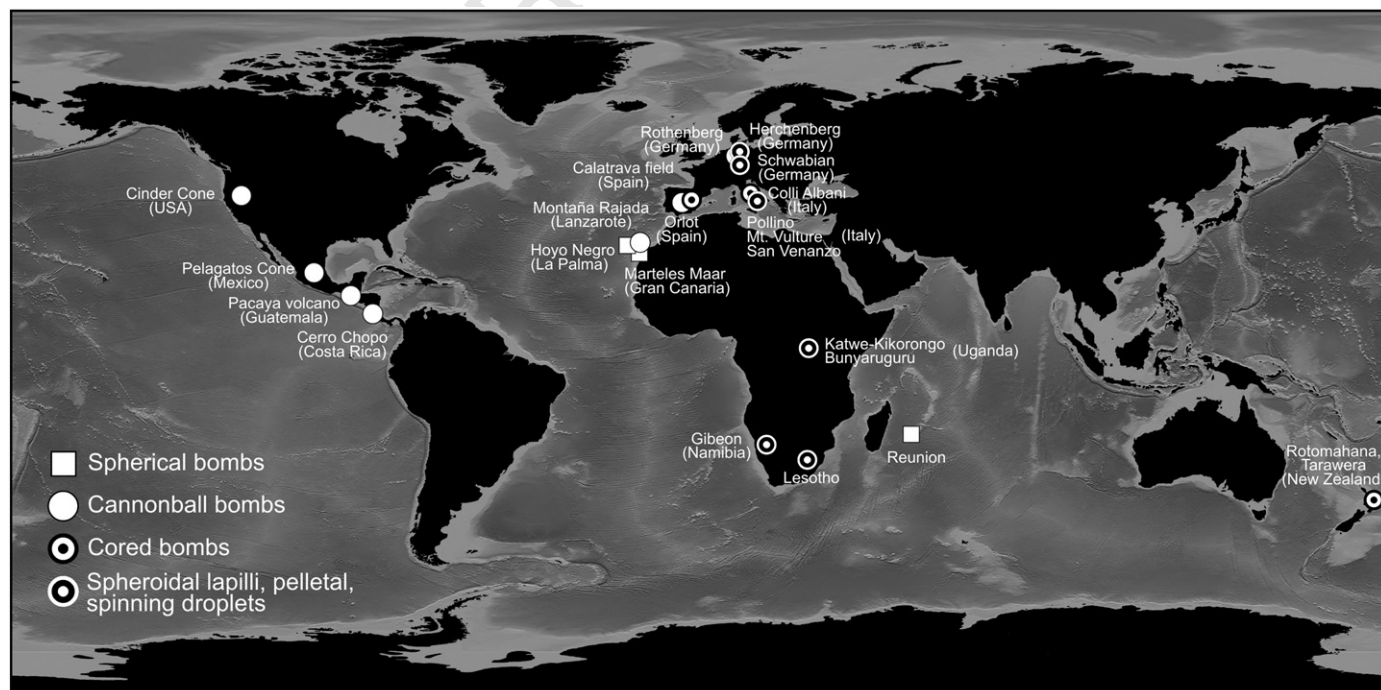


Fig. 12. Volcanoes in the world with reported spherical bombs and its variations (for references, see the text).

Schmincke, 1984). At Chopo, an island arc tholeiitic basalt, the comagmatic component in the bombs is omnipresent, and no example of cored bombs was found.

At Pelagatos scoria cone in Mexico there are abundant broken and rough bombs and the clasts range from dense angular to vesicular, in contrast to the abundant cannonball bombs and lapilli at Chopo. The range of vesicularity in the coarse juvenile clasts is wide and bimodal (60–80 vol.% and 5–20 vol.%, Guilbaud et al., 2009), and lesser in Chopo (5–40 vol.%), so the recycling process must have played a subordinate role at Pelagatos, where the main part of the beds often displays normal grading at the top (Guilbaud et al., 2009). The gradation at Cabezo Segura volcano is variable, being occasionally reverse and less often normal with a clast- to matrix-supported fabric (Carracedo Sánchez et al., 2009), in contrast with our case study where reverse grading is present all through the deposits.

Compositionally, all cases of spherical bombs are related to mafic and ultramafic magmas with low to moderate viscosity and high-temperature; and a few of them are related to subduction settings. In addition, most of the spherical bomb examples are from intraplate volcanism (Fig. 14), including alkaline picobasalts and basanites at the Calatrava volcanic field (Carracedo Sánchez et al., 2009), basanitic at Marteles and Hoyo Negro vents (Schmincke, 1977; Schmincke and Sumita, 2010), alkaline basalts at Montaña Rajada (Carracedo and Rodríguez, 1991), tephritic to basanitic at Rothenberg cone (Houghton and Schmincke, 1989), and tephrite to K-foidite in Colli Albani Volcanic District (Roman, Italy; Sottili et al., 2009). Equivalent spheroidal lapilli (composite lapilli, pelletal lapilli and spinning droplets), are restricted to mafic to ultramafic, silica undersaturated eruptive magmas (Bednarz and Schmincke, 1990; Lloyd and Stoppa, 2003; Carracedo Sánchez et al., 2009). However, a few basaltic examples associated with subduction volcanism are observed as is the case of Pacaya volcano and the Rotomahana eruption of Tarawera (Francis, 1973; Rosseeil et al., 2006, respectively), high-Mg basaltic andesite at Pelagatos (Guilbaud et al., 2009), and basaltic tholeiite at Chopo (present work).

6. Conclusions

The primary external water source for the phreatomagmatic eruption during the early stages of Chopo is assumed to be an aquifer hosted in the 8-m-thick deposit of underlying Lower Pleistocene andesitic lavas. This phreatomagmatic event probably constructed a small tuff ring. Then something led to a decrease in the water supply, which might be an upwards migration of the fragmentation level, away from the aquifer depth, or an increase of the magma discharge rate. Thus, during the short period of activity at Chopo cone there is a well documented drastic decrease of the hydromagmatic character, replaced by the occurrence of a more magmatic event. The pyroclastic cone is atypical relative to well known scoria cones in that it contains juvenile clasts with low vesicularity (5–40 vol.%), and pervasive reverse-graded pyroclastic deposits. The range of juvenile clast vesicularity is interpreted here to be a consequence of an open-vent system, allowing various degassing levels and partial blockages of the vent. The reverse-graded sequences around the cone are interpreted mainly as lateral grain movement, although there might have existed varying conditions at the vent that resulted in lower explosivity and less efficient fragmentation at the beginning of each pulse.

Cannonball bombs and lapilli are very abundant at Chopo; they are interpreted as the complex result of differences in residence times and degassing stage of magma pulses, the cyclical declining supply of fresh gas-rich magma, leading to lava stagnation and decreasing vigor of the explosions, in addition to the recycled through the vent and the flight (= cooling time), until they finally land on the high steep flanks, rolling and rounding down the slopes.

7. Uncited reference

Morris and Hart, 1983

Acknowledgements

The Instituto Costarricense de Electricidad (ICE) is specially acknowledged for the logistical support of this work. Special mentions go to F. Arias, D. Boniche, and R. Monge who gave generous assistance during the field and laboratory investigations, and to the Laboratorio de Ingeniería Geotécnica for the density measurements. H. R. Gröger is grateful to the Deutsche Akademische Austauschdienst (DAAD) for a grant allowing her to stay in Costa Rica and part of the fieldwork. R. Hannah provided the electron microprobe analyses. D. Szymanski, K. Stockstill, C. Webster, E. Wilson, C. Corrigan and M. Feigenson helped in the very early version of the petrochemistry section. M.J. Carr provided the early reference of Darwin about the spherical bombs, and C. Romero to show to GEA the cannonball tephra locality at Timanfaya. We are also grateful to Brittany D. Brand and Gianluca Sottili for meaningful reviews of the manuscript.

References

- Araña, V., López, J., 1974. Volcanismo. Dinámica y Petrología de sus Productos, Ed. Istmo, Madrid. 757
- Bacon, C.R., 1990. Calc-alkaline, shoshonitic, and primitive tholeiitic lavas from monogenetic volcanoes near Crater Lake, Oregon. J. Petrol. 31, 135–166. 758
- Bagnold, R.A., 1954. Experiments on a gravity-free dispersion of large solid spheres in a Newtonian fluid under shear. Proc. R. Soc. Lond. 1160, 49–63. 761
- Bateman, P.C., 1953. Up-side-down graded bedding in right-side-up lacustrine pumice (California). Geol. Soc. Amer. Bull. 64, 1499–1500. 762
- Bates, R.L., Jackson, J.A., 1987. Glossary of Geology. American Geological Institute, Alexandria. 765
- Bednarz, U., 1982. Geologie und Petrologie der spätquartären Vulkane Herchenberg, Leilenkopf und Dümpelmaar (nördliches Laacher-See-Gebiet). Diplom Thesis, Ruhr-Universität Bochum, Germany. 767
- Bednarz, U., Schmincke, H.-U., 1990. Evolution of the Quaternary melilite–nephelinite Herchenberg volcano (East Eifel). Bull. Volcanol. 52, 426–444. 771
- Blackburn, E.A., Wilson, L., Sparks, R.S.J., 1976. Mechanisms and dynamics of Strombolian activity. J. Geol. Soc. Lond. 132, 429–440. 772
- Booth, B., 1973. The Granadilla pumice deposit of southern Tenerife, Canary Islands. Proc. Geol. Assoc. Lond. 84, 353–370. 774
- Breed, W.J., 1964. Morphology and lineation of cinder cones in the San Francisco volcanic field. Mus. N. Ariz. Bull. 40, 65–71. 777
- Brewer, R., 1964. Fabric and Mineral Analysis of Soils. John Wiley & Sons, London and New York. 778
- Bryan, W.B., Finger, L.E., Chayes, F., 1969. Estimating proportions in petrographic mixing equations by least-squares approximations. Science 163, 926–927. 780
- Carracedo, J.C., Rodríguez, E., 1991. Lanzarote. La erupción volcánica de 1730. Servicio de Publicaciones, Cabildo Insular de Lanzarote. 782
- Carracedo Sánchez, M., Sarrionandia, F., Arostegui, J., Larrondo, E., Ibarguchi, J.I., 2009. Development of spheroidal composite bombs by welding of juvenile spinning and isotropic droplets inside a mafic eruption column. J. Volcanol. Geotherm. Res. 186, 265–279. 784
- Cas, R.A.F., Wright, J.V., 1987. Volcanic Successions, Modern and Ancient. Allen & Unwin, London. 788
- Chiesa, S., Alvarado, G.E., Pecchio, M., Corella, M., Sanchi, A., 1994. Contribution to petrological and stratigraphical understanding of the Cordillera de Guanacaste lava flows. Costa Rica. Rev. Geol. Amér. Cent. 17, 19–43. 792
- Darwin, C., 1845. Journal of Researches into the Natural History and Geology of the Countries Visited during the Voyage of H.M.S. Beagle round the World, under the Command of Capt. Fitz Roy. R.N. John Murray, London. 793
- Duffield, W.A., Bacon, C.R., Roquemore, G.R., 1979. Origin of reverse-graded bedding in air fall pumice, Coso Range, California. J. Volcanol. Geotherm. Res. 5, 35–48. 796
- Denyer, P., Alvarado, G.E., 2007. Mapa Geológico de Costa Rica. -Librería Francesa S.A., 1: 400000. 799
- Feigenson, M.D., Carr, M.J., 1993. The source of Central American lavas: inferences from geochemical inverse modeling. Contrib. Mineral. Petrol. 113, 226–235. 800
- Fisher, R.V., Schmincke, H.-U., 1984. Pyroclastic Rocks. Springer Verlag, Berlin, New York. 802
- Francis, P.W., 1973. Cannonball bombs, a new kind of volcanic bomb from the Pacaya Volcano. Guatemala. Geol. Soc. Amer. Bull. 84, 2791–2794. 804
- Francis, P., Oppenheimer, C., 2004. Volcanoes. Oxford Univ. Press. 806
- Guilbaud, M.-N., Siebe, C., Agustín-Flores, J., 2009. Eruptive style of the young high-Mg basaltic-andesite Pelagatos scoria cone, southeast of México City. Bull. Volcanol. 71, 859–880. 808
- Hannah, R.S., Vogel, A.T., Patiño, L.C., Alvarado, G.E., Perez, W., Smith, D.R., 2000. Origin of silicic volcanic rocks in Central Costa Rica: a study of a chemically variable ash-flow sheet in the Tiribí Tuff. Bull. Volcanol. 64, 117–133. 810
- Hart, W.K., Aronson, J.L., Mertzman, S.A., 1984. Aerial distribution and age of low-K, high-alumina olivine tholeiite magmatism in the northwestern Great Basin. Bull. Geol. Soc. Amer. 95, 186–195. 812
- Hasenaka, T., Carmichael, I.S.E., 1987. The cinder cones of Michoacán–Guanajuato, Central Mexico: petrology and chemistry. J. Petrol. 28, 241–269. 816

- 818 Heiken, G., 1978. Characteristics of tephra from Cinder Cone, Lassen Volcanic National
819 Park. California. *Bull. Volcanol.* 41, 119–130.
- 820 Herrstrom, E.A., Reagan, M.K., Morris, J.D., 1995. Variations in lava composition
821 associated with flow asthenosphere beneath southern Central America. *Geology*
822 23, 617–620.
- 823 Houghton, B.F., Hackett, W.R., 1984. Strombolian and phreatomagmatic deposits of
824 Ohakune craters, Ruapehu, New Zealand: a complex interaction between external
825 water and rising basaltic magma. *J. Volcanol. Geotherm. Res.* 21, 207–231.
- 826 Houghton, B.F., Schmincke, H.-U., 1989. Rothenberg scoria cone, East Eifel: a complex
827 Strombolian and phreatomagmatic volcano. *Bull. Volcanol.* 52, 28–48.
- 828 Houghton, B.F., Wilson, C.J.N., 1989. A vesicularity index for pyroclastic deposits. *Bull.*
829 *Volcanol.* 51, 451–462.
- 830 Houghton, B.F., Wilson, C.J.N., Pyle, D.M., 2000. Pyroclastic fall deposits. In: Sigurdsson,
831 H., Houghton, B., McNutt, S., Rymer, H., Stix, J. (Eds.), *Encyclopedia of Volcanoes*.
832 Academic Press, San Diego, pp. 555–570.
- 833 Kokelaar, B.P., 1986. Magma–water interactions in subaqueous and emergent basaltic
834 volcanism. *Bull. Volcanol.* 48, 275–290.
- 835 Krumbein, W.C., 1941. Settling velocity and flume-behaviour of non-spherical particles.
836 *Trans. Am. Geophys. Union* 621–633.
- 837 Lautze, N.C., Houghton, B.F., 2005. Physical mingling of magma and complex eruption
838 dynamics in the shallow conduit at Stromboli volcano, Italy. *Geology* 33, 425–428.
- 839 Lirer, L., Pescatore, T., Booth, B., Walker, G.P.L., 1973. Two Plinian pumice-fall deposits
840 from Somma–Vesuvius. Italy. *Geol. Soc. Amer. Bull.* 84, 759–772.
- 841 Lloyd, F.E., Stoppa, F., 2003. Pelletal lapilli in diatremes – some inspiration from the old
842 masters. *Geolines* 15, 65–71.
- 843 Macdonald, G.A., 1972. *Volcanoes*. Prentice-Hall Inc.
- 844 Mangan, M.T., Cashman, K.V., 1996. The structure of basaltic scoria and reticulate and
845 inferences for vesiculation, foam formation, and fragmentation in lava fountains.
846 *J. Volcanol. Geotherm. Res.* 73, 1–18.
- 847 McGetchin, T.M., Settle, M., Chouet, B.A., 1974. Cinder cone growth modeled after
848 Northeast Crater, Mount Etna, Sicily. *J. Geophys. Res.* 79, 3257–3272.
- 849 McKnight, S.B., Williams, S.N., 1997. Old cinder cone or young composite volcano?: the
850 nature of Cerro Negro, Nicaragua. *Geology* 25, 339–342.
- 851 Mora, S., 1977. Estudio geológico del Cerro Chopo. *Rev. Geográf. Amér. Cent.* 5–6,
852 189–199.
- 853 Morris, J.D., Hart, S.R., 1983. Isotopic and incompatible element constraints on the
854 genesis of island arc volcanics from Cold Bay and Amak Island, Alutains and
855 implications for mantle structure. *Geochim. Cosmochim. Acta* 47, 2015–2033.
- 856 Murata, K.J., Dóndoli, C., Sáenz, R., 1966. The 1963–65 Eruption of Irazú Volcano, Costa
857 Rica (the period of March 1963 to October 1964). *Bull. Volcanol.* 29, 765–796.
- 858 Parfitt, E.A., Wilson, L., 1995. Explosive volcanic eruptions—IX. The transition between
859 Hawaiian-style lava fountaining and Strombolian explosive activity. *Geophys. J. Int.*
860 121, 226–232.
- 861 Ramírez, O., Umaña, J., 1977. Proyecto Corobicí. Informe Geológico de Viabilidad.
862 Unpublished internal Report, Instituto Costarricense de Electricidad, Dept.
863 Geología.
- 864 Rittmann, A., 1960 (2 ed.). *Vulkane und ihre Tätigkeit*. F. Enke, Stuttgart.
- 865 Rosseel, J.B., White, J.D.L., Houghton, B.F., 2006. Complex bombs of phreatomagmatic
866 eruptions: role of agglomeration and welding in vents of the 1886 Rotomahana eruption,
867 Tarawera, New Zealand. *J. Geophys. Res.* 111, B12205. doi:10.1029/2005JB004073.
- Schmincke, H.-U., 1977. Phreatomagmatische Phasen in quartären Vulkanen der
868 Osteifel. *Geol. Jb A39*, 1–48. 869
- Schmincke, H.-U., Sumita, M., 2010. Geological evolution of the Canary Islands. A Young
870 Volcanic Archipelago Adjacent to the Old African Continent. Gorres-Druckerei und
871 Verlag GMBH, Koblenz. 872
- Sohn, Y.K., Kim, S.B., Hwang, I.G., Bahk, J.J., Choe, M.Y., Chough, S.K., 1997. 873
874 Characteristics and depositional processes of large-scale gravelly Gilbert-type
875 foresets in the Miocene Downsman fan delta, Pohang basin, SE Korea. *J. Sed. Res.* 67,
876 130–141. 877
- Sottili, G., Taddeucci, J., Palladino, D.M., Gaeta, M., Scarlato, P., Ventura, G., 2009. Sub-
878 surface dynamics and eruptive styles of maars in the Colli Albani Volcanic District,
879 Central Italy. *J. Volcanol. Geotherm. Res.* 180, 189–202. 880
- Sottili, G., Taddeucci, J., Palladino, D.M., 2010. Constraints on magma–wall rock thermal
881 interaction during explosive eruptions from textural analysis of cored bombs.
882 *J. Volcanol. Geotherm. Res.* 192, 27–34. 883
- Sun, S.S., McDonough, W.F., 1989. Chemical and isotopic systems of oceanic basalts:
884 implications for mantle composition and processes. In: Saunders, A.D., Norry,
885 M.J. (Eds.), *Magmatism in the Ocean Basins*: Geol. Soc. Lond. Spec. Pub., vol. 42,
886 pp. 313–345. 887
- Tatsumi, Y., Hamilton, D.L., Nesbitt, R.W., 1986. Chemical characteristics of fluid phase
888 from the subducted lithosphere: evidence from high pressure experiments and
889 natural rocks. *J. Volcanol. Geotherm. Res.* 29, 293–309. 890
- Tournon, J., 1984. Magmatismes du mesozoïque à l'actuel en Amérique Centrale:
891 L'exemple de Costa Rica, des ophiolites aux andésites. Ph.D. Thesis, Mem. Sc. Terre,
892 Univ. Curie, Paris. 893
- Valentine, G.A., Gregg, T.K.P., 2008. Continental basaltic volcanoes – processes and
894 problems. *J. Volcanol. Geotherm. Res.* 177, 857–873. 895
- Vergnolle, S., Brandeis, G., 1996. Strombolian explosions 1. A large bubble breaking at
896 the surface of a lava column as a source of sound. *J. Geophys. Res.* 101,
897 20433–20447. 898
- Vergnolle, S., Brandeis, G., Mareschal, J.-C., 1996. Strombolian explosions 2. Eruption
899 dynamics determined from acoustic measurements. *J. Geophys. Res.* 101,
900 20,449–20,466. 901
- Walker, G.P.L., Croasdale, R., 1972. Characteristics of some basaltic pyroclastics. *Bull.*
902 *Volcanol.* 35, 303–317. 903
- Williams, H., McBirney, A.R., 1979. *Volcanology*. Freeman, Cooper & Co, San Francisco. 904
- Wilson, L., 1976. Explosive volcanic eruptions—II. Plinian eruption columns. *Geophys. J.*
905 *Roy. Astron. Soc.* 45, 543–556. 906
- Wohletz, K.H., 1999. *MAGMA: Calculates IUGS Volcanic Rock Classification, Densities,*
907 *and Viscosities. Los Alamos National Laboratory Computer Code LA-CC 99-28, Los*
908 *Alamos New Mexico.* 909
- Wolff, J.A., Sumner, J.M., 2000. Lava fountains and their products. In: Sigurdsson, H.,
910 Houghton, B., McNutt, S., Rymer, H., Stix, J. (Eds.), *Encyclopedia of Volcanoes*.
911 Academic Press, San Diego, pp. 321–329. 912
- Wood, C.A., 1980. Morphometric evolution of cinder cones. *J. Volcanol. Geotherm. Res.*
913 7, 387–413. 914
- Wright, H.M.N., Cashman, K.V., Rosi, M., Cioni, R., 2007. Breadcrust bombs as indicators
915 of Vulcanian eruption dynamics at Guagua Pichincha volcano, Ecuador. *Bull.*
916 *Volcanol.* 69, 281–300. 917
- Zingg, T., 1935. Beitrag zur Schotteranalyse. *Schweiz Min. Petrog. Mitt.* 15, 39–140. 917